SYNERGISTIC EFFECTS OF COMBINING THERAPEUTIC RADIATION AND β-LAPACHONE AGAINST TUMORS

A DISSERTATION SUBMITTED TO

THE FACULTY OF THE GRADUATE SCHOOL

OF

THE UNIVERSITY OF MINNESOTA

BY

TROY ANTONIO DOS-SANTOS, Ph.D.

IN PARTIAL FULFILMENT OF THE REQUIREMENTS

FOR THE DEGREE OF

DOCTOR OF PHILOSOPHY

PROFESSOR CHANG WON SONG, ADVISER

DECEMBER 2013

Acknowledgements

It is with great humility and honesty that I graciously recognize that without the generous efforts of many other outstanding individuals, this completed work, as represented by this dissertation, would not have been possible. The following is a partial list of the more notable individuals; the short nature of these acknowledgements is under-representative of the full extent of their contributions. I would like to give my deep thanks to my advisor, Dr. Chang Song. His many years of acclaimed scientific scholarship, and his broad accumulated experience in the field of radiation physics and cancer radiobiology, and life in general, has been a tremendous opportunity for me to learn and grow both academically and in life. I am forever grateful for the knowledge and strengthening experiences bestowed upon me during my time as an advisee. I would like to thank Dr. Susanta Hui for generously providing his time and energies in mentorship and professional guidance. While being a young scientist already of high caliber and note, Dr. Hui has also never forgotten the path he took while being a student, and as such, his mentorship and encouragements resonated well, and has been remembered. Sterling Mikkelson, John Powers and Dr. Omolara Lawani have countless times proven themselves indispensable, not only in assisting both in vitro and in vivo experiments, which required several reliable and skilled experimenters, but also due to their attention to detail, many potential experimental errors have been adverted while improved techniques have been introduced; to them I owe my tremendous gratitude. Without the patient teaching of both Kaoru Terai and Genya Gekker, my most challenging set of experiments, protein immunoblot analysis and flow cytometry analysis respectively, would have remained insurmountable. Finally, I acknowledge Karina Lawrence's professional administrative support and timely laboratory supplies which kept the laboratory functioning smoothly.

Dedication

This work is dedicated to my family who have loved and supported me throughout the years without prerequisite.

Abstract

Understanding the mechanisms of the experimental anti-cancer drug β-Lapachone is crucial for optimizing its mode of action - especially when it is used in conjunction with other treatment regimens, namely therapeutic radiation, due to possible interactions. It is our aim to exploit the knowledge gained from studying the interaction between β-Lapachone and radiation for better tumor control. β-Lapachone is a novel anti-cancer compound that is activated intracellularly by the enzyme NAD(P)H:quinone oxidoreductase 1 (NQO1), which is over-expressed in many cancer cells. It has been reported that concentrations of NQO1 can be further up-regulated by various cellular stressors including radiation. Therefore radiation potentiates β-Lapachone's cytotoxicity when radiation is used as a pre-treatment. Treating with β-Lapachone in fractionated radiation treatments, have been shown to suppress sub-lethal damage (SLD) repair of radiation damage. Therefore combined treatments of radiation and β-Lapachone have been observed to involve synergistic interactions based on two complementary actions: pretreatment of cancer cells with radiation to increase NQO1 which potentiate β-Lapachone's cytotoxicity and suppression of SLD repair by β-Lapachone post irradiation. In an attempt to illuminate important factors for designing an optimal treatment for solid tumor control, a deeper understanding of the interactions between the two treatments was needed, such as, the changes made in the cell cycle of several cell lines by various treatment combinations involving radiation and β-Lapachone, changes made in the concentrations of NQO1 pre/post-treatments involving β-Lapachone, and the impact of treatment on the tumor micro-environment in regards to in vivo tumor response to fractionated radiation in the presents of β-Lapachone. Our results shows a marked sensitization towards radiation of FSaII and A549 cells treated with β-Lapachone and a significant suppression of sub-lethal damage (SLD) repair. β- Lapachone's cytotoxicity appears to be agnostic towards cell cycle phase and hypoxic cells. β- Lapachone has also been shown to be effective in delaying growth of FSaII tumors grown in C3H mice when treated in a single β-Lapachone dose and a single fraction of radiation as opposed to its fractionated regimen analog, and so placing it as a candidate for steriotatic body radiation therapy (SBRT) and steriotatic radiosurgery (SRS) combined treatments.

Table of Contents

List of Tables

List of Figures

1 Introduction

As one of the oldest documented diseases in history, cancer is first known to be described more than 5000 years ago (1), and is believed to have existed for all of human history. Hippocrates (ca. 460 BC – ca. 370 BC) however was responsible for coining the term. It is only in recent history, with the invention of the microscope and a fuller understanding of physiology, we understand the cellular basis of cause and progression of cancers and tumors.

1.1 Cancer Prognosis with Radiation Therapy: Then and Now

The established modalities of cancer treatment in medicine include localized treatments such as surgery and radiation therapy, and systemic treatments such as chemotherapy, hormonal therapy, autoimmune therapy, and radioactive particle uptake therapy. Surgery was the first modality used successfully in the treatment of cancer. As predictive abilities in relation to genetics and behavior are improved, prophylactic surgery has become a growing treatment path; notably women having a mutated BRCA-1 gene being at high risk for developing breast cancer are electing to have a double breast mastectomy (2) (3). Unlike surgery, cancer treatment with chemotherapy is systemic and is the main treatment available for disseminated malignant diseases. A wide verity of chemical agents have been identified and successfully used to treat cancer. Two main classes of chemotherapeutic drugs are either cell cycle phase specific or phase non-specific. In short, phase specific indicated that above a certain dosage level, further

increase in drug doesn't result in more cell killing and in the case of phase non-specific, the drugs generally have a linear (or exponential) dose-response curve. As has been mentioned before, chemotherapy is a systemic treatment, as such the modality of choice for certain non-localized cancers among others, but this ability to have access to all cancerous cells in the body also means equal access to all health cells, paving the way for unintended side-effects through the targeting of healthy cells. The side effects of many chemotherapy drugs are well known and documented, including nausea and hair loss being among the most notable. Of greater interest in this dissertation is the application of radiation for the treatment of tumors, notably its application in conjunction with chemotherapeutic agents.

Radiation therapy is a local modality used in the treatment of cancer. Upon its discovery by Wilhelm Röntgen, "On a new kind of rays" (4), 'x'-rays were very quickly exploited for its medical potential (5). Radiation therapy is one of the most important modalities for the treatment of cancer. According to the Physician Characteristics and Distribution in the U.S. (2008 Edition, 2004 IMV Medical Information Division, 2003 SROA Benchmarking Survey), nearly two-thirds of all cancer patients received radiation therapy. In 2004, nearly one million patients in the U.S. were treated with radiation therapy, that sixty percent of the patients treated in 2004, or 574,930 individuals, had not previously received radiation therapy. In 2004 about 23.4 million patients visited hospitals and freestanding radiation therapy centers. Three cancers – breast cancer, prostate cancer and lung cancer – make up more than half (56 percent) of all patients receiving radiation therapy. For most cancer types treated with radiation therapy, at least 75 percent of the patients are treated with the intent to cure the cancer, rather than control

the growth or relieve symptoms like pain. For lung and brain cancers, that number is somewhat lower, with 59 percent of lung cancer patients and 50 percent of brain cancer patients being treated with the goal of curing the cancer. In 2004, 88 percent of patients treated with radiation therapy received external beam x-rays treatments from a linear accelerator with more specialized radiation treatments such as Gamma Knife and brachytherapy (using radioactive sources) make up the remaining 12 percent.

Success of radiotherapy treatment largely depends on the differences in the radiosensitivity between the tumor and normal tissue and this will be discussed in detail below. Although x-rays are the primary radiation source for treatments, radionuclides have been used locally in the case of brachytherapy and gamma knife, and systemically to treat systemic malignant disorders. Of note in radionuclide systemic treatments, radioactive iodine is the treatment of choice for thyroid cancer while strontium-89 tritiated with simple sugars is used for the treatment of metastasis.

Prognosis due to medical intervention has been improving in recent years, though very slowly. Despite the wealth of knowledge regarding cancer, and improved detection and treatment, many types of cancers have hardly made a budge as far as the 5 year relative cancer survival rate. The relative cancer survival rate is a specific measurement of survival where the rate is calculated by adjusting the rate to remove all causes of death except cancer. It is the ratio of a cancer patient's chance of surviving a given time interval to that of an average person of the same age and sex (6). As can be seen in Figure 1.1.a, there haven’t been significant improvement in cancer mortality in relation to lung and bronchus cancers, where patients from 2003-2007 have not shown significant improvement above the last date points shown in Figure 1.1.a (6). On a positive note

however, while improvements in prognosis have incrementally improved, there is a steady and consistent increase in survival, indicating that, among other factors such as improved lifestyle and early detection, research efforts are having a positive impact on cancer prognosis. It is my hope that the work completed, as summarized by this dissertation, aids in this effort to improve and increase the scientific community understanding of cancer and its treatment.

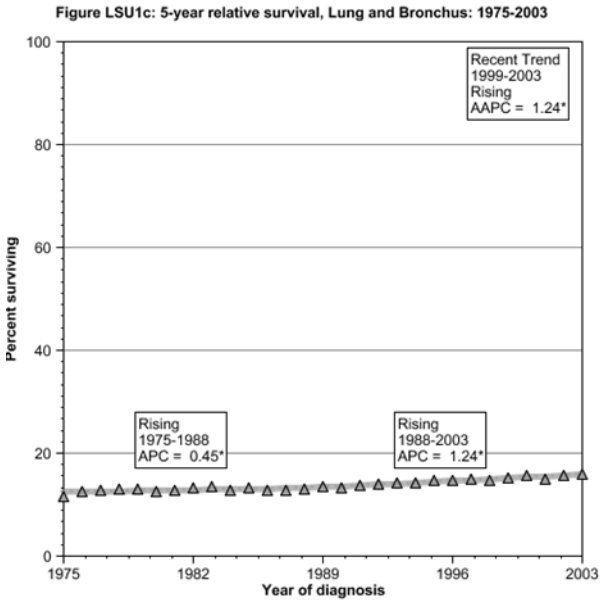

Figure 1.1.a Percent 5-year relative survival of lung and bronchus cancer patients. Source: Cancer Trends Progress Report—2011/2012 Update, National Cancer Institute, NIH, DHHS, Bethesda, MD, April 2010, http://progressreport.cancer.gov

1.2 Irradiation of Living Cells

Radiation generally refers to the physical property of many different forms of energy departing an atom. One of two ways to broadly classify radiation is to consider whether the radiation has its origins within the nucleus or not, while the other being

whether it is a particle (Fermions) or an electromagnetic photon (Boson).

Common Types of Radiation	Atomic Source	Fundamental Nature (Boson or Fermions)
Alpha	Nuclear	Fermions
X-rays	Electronic Configuration	Boson
Beta	Nuclear	Fermions
Neutron	Nuclear	Fermions
Gamma	Nuclear	Boson

Table 1.2.a. Examples of common types of radiation showing its respective atomic source and fundamental nature.

When radiation interacts with a material other than its source, its energy determines whether it has the ability to ionize; namely have the energy to liberate an electron (or any other atomic component such as part of or the whole nucleus) from an atom or molecule. Radiation having sufficient energy to liberate parts of an atom from its original form, thereby creating charged particles, is known as ionizing radiation, conversely, radiation having only sufficient energy to change the energy states associated with the rotational, vibrational or electron valence configurations of atoms and molecules, is called non-ionizing radiation.

Radiobiology seeks to understand the biologic response of living cells to ionizing radiation, and for practical considerations, the greatest emphasis have been placed on understanding the biologic response to therapeutically relevant radiation. Specifically, the entity within a cell that leads to the most significant biologic response is the DNA molecule. However, while x-rays dominate radiotherapy, technological improvements have made other radiation modalities more and more feasible. First example is fast

neutrons – the hammersmith cyclotron was suggested and conceived by Gray based on the notion that a lowered OER would be beneficial in radiotherapy. The cyclotron, however, suffered from the limitations of poor depth doses (equivalent to 250-kVp x-rays) and a fixed horizontal beam. Cyclotrons built for neutron therapy achieved good dose depth but suffered from high radiation toxicity due to its high relative biological effectiveness. All had fixed horizontal beams, and all were located in physics building far away from patients. Boron-neutron capture theory – the idea is to deliver to the cancer patient a boron-containing drug that is taken up only in tumor cells and then exposes the tumor cells to sublethal neutron therapy. When the neutron interacts with the boron, the boron will emit densely ionizing short- range alpha particles to the tumor. However, to date there are no boron containing chemical agents that can be selectively up-taken into the tumor, additionally, low energy neutrons have poor depth doses. Protons – the OER is almost indistinguishable from that of x-rays. The dose deposited by a beam of protons increases slowly with depth, but reaches a sharp maximum near the end of the range of the Bragg peak. Proton beams ranging in energy from 150 to 200 MeV are of interest in radiotherapy because this corresponds to ranges of about 16-26 cm in tissue. Interest in carbon ion radiotherapy has been rekindled largely in Europe and Japan. The characteristic depth-dose profile of heavy ions, which is similar to that of protons, is very attractive for the radiotherapy of deep-seated tumors. The depth at which the peak occurs depends on the energy. The peak is so narrow that it must be ‘spread out’ by varying the energy of the beam. Compared with protons, carbon ions have less lateral scattering, leading to shaper beam edges.

The amount of ionizing events within an irradiated cell is directly related to its

biologic response. Quantifying the amount of ionizing events within such a cell is known as the dose, which is the charge, measured in the SI unit of Coulomb (C), of the ionized particles produced per unit mass is the absorbed energy. The modern unit for measured absorbed energy in tissue is the Gray (Gy), which is defined as the 1 Joule (J) of deposited energy in 1 kilogram (kg) of tissue. The first unit for measuring dose was the roentgens (R) which was standardized to measurement of dose to air, where a conversion factor was needed to account for the dose to tissue (or any other target material), the resulting adjusting dose was known simply as the rad.

$$1\ \frac{\mathrm{C}}{\mathrm{kg}} = 3876\ \mathrm{R} \cong 3720.96\ \mathrm{rad\ (in\ soft\ tissue)}$$

$$1\ \mathrm{rad} = 0.01\ \frac{\mathrm{J}}{\mathrm{kg}} = 0.01\ \mathrm{Gy}$$

The energy of the radiation needed to cause ionizing events is hard to define and quantify in the form of a dose, due to the fact that there are several different forms of ionizing radiations, that the specific type of interaction (photoelectric effect, compton scattering or pair production) is radiation energy dependent in the case of photons, that the target material, more specifically living tissue, is comprised of a verity of atoms and molecules and as such have a range of ionizing energies, that the newly ionized charged particles go on the cause other ionizing events, etc., however, the first electronic ionizing energy for both hydrogen and oxygen (the atomic constitutions of water, where water is by orders of magnitude the most abundant molecule within a cell) are 14 eV, this can be considered the minimum incoming radiation energy each photon needs to cause an ionizing event in tissue. Simplifying this problem by assuming soft tissue to have a 100% composition of water, then determining the likelihood of interactions, and their frequency

can now more easily be determined.

Photon Energy	Relative Number of Interactions (%)		
(MeV)	τ	σ	π
0.01	95	5	0
0.026	50	50	0
0.06	7	93	0
0.15	0	100	0
4	0	94	6
10	0	77	23
24	0	50	50
100	0	16	84

Table 1.2.b Relative importance of photoelectric (τ), Compton (σ), and pair production (π) in water (7).

There are also marked differences in how a photon (X- ray) and a particle deposits their energy with-in tissue, where what distinguishes the two have biological implications. Radiation tend to have a more direct ability to ionize atoms or molecules which can cause a biologic effect, while photons tend to deposit its energy less frequently over a longer distance.

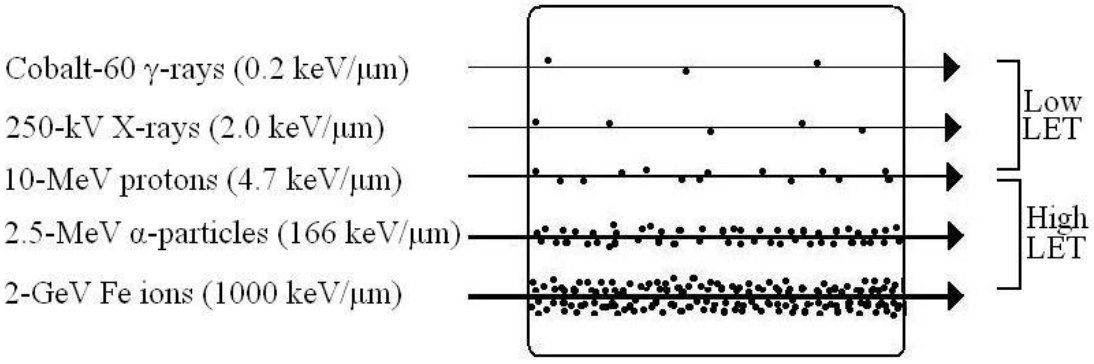

Figure 1.2.c Visual depiction of the linear energy transfer (LET) per unit length among different types of radiation. Each dot indicates an ionizing event. Low LET radiation is considered lightly ionizing while high LET is considered densely ionizing.

While there are caveats regarding radiative LET, such as its energy deposition are distance-traveled dependent, the biologically relevant information relates to whether it is able to directly or indirectly ionize atoms or molecules which lead to biologically relevant changes. In the case of directly ionizing radiation, the probability that such a particle can ionize a cell's atom or molecule leading to a biologic response is much higher than the case where the ionized product of a non-biologically relevant atom or molecule is itself the ionizing agent acting on a cell's atom or molecule that has the potential of a biologic response, notably DNA. Most commonly, the indirect ionizing reaction achieves its energy deposition through the creation of free radical ions by the very ions created from ionizing intra-cellular water molecules.

$$H_2O + \text{ϟ} \rightarrow H_2O^+ + e^-$$

$$H_2O + H_2O^+ \rightarrow H_3O^+ + OH^-$$

When an incident externally originating x-ray photon having at least 14 eV (represented by "ϟ") ionizes a water molecule, which constitutes 80% of a living cell, it may become ionized resulting in H_2O^+ and a free electron would have been produced. In the case for H_2O^+, if it meets another water molecule within its short lifetime of 10-10 seconds, it can react with it to form a hydronium ion, H_3O^+, and a highly reactive hydroxyl radical, OH^-, which can diffuse more than twice the length of the diameter of a DNA double helix (8).

Survival of Irradiated Cells

Radiation damage to the DNA leads to a greater biological response, when compared to an equivalent radiation dose to other cellular organelles. It only takes between 1 and 2 Gy to cause sufficient DNA damage that will result in the loss of

clonogenic potential; where clonogenic potential refers to a cancerous cell's ability to proliferate indefinitely.

Irradiated cells die most often at mitosis (9) (10) (11) (12) (13). The best method for determining the effect of irradiation on cell survival is to measure the number of cells with the potential to divide indefinitely. That is, the 'clonogenic assay' is the best measure for cells with the potential to divide indefinitely, most importantly because this assay allows time for the survival cells to cycle through many cycles in an effort to separate the clonogenically viable cells from the mortally damaged cells that will survive for several generation but eventually die.

According to target therapy, the survival of cells exponentially decrease with a linear increase in high-LET radiation dose, as such the surviving fraction (SF) of cells can be modeled as:

$$\mathrm{SF} = \mathrm{e}^{-\alpha \mathrm{D}}$$

Where -α is the slope and D is the radiation dose, when the SF is plotted on a log scale. If we assume that each ionizing event results in loss of clonogenic potential and also assume that each cell has a single target (DNA), then we can use Poission's statistics to determine the probability of an ionizing event that will lead to loss of clonogenic potential.

$$P(n) = \frac{e^{-x} x^{n}}{n!}$$

Where x is the average number of events and n is the specific number of events. (If each ionizing event results in loss of clonogenic potential (x = 1), then the probability of survival is the probability of not being ionized (n = 0). From the Poisson statistics we would have:

$$P(0) = \frac{e^{-1} \cdot 1^0}{0!} = e^{-1} = surviving\ fraction\ of\ 0.368\ or\ \sim 37\%$$

If $D_0 = 1 / \alpha$, then

$$SF = e^{-\alpha D} = e^{-D/D0}$$

So when $D_0 = D$, then

$$e^{-1} = surviving\ fraction\ of\ 0.368\ or\ \sim 37\%.$$

Therefore, D_0 is often called the mean lethal dose, or the dose that, on average, causes the loss of clonogenic potential per cellular target.

In preparation for characterizing the radiation response of rodent fibrosarcoma cells (FSaII) of the C3H mice, the following clonogenic assay was performed. FSaII cells were harvested, using 0.25% of a digestive enzyme solution, trypsin, containing ethylenediaminetetraacetic acid (EDTA) for 5 minutes at 37ºC, while they were in an exponential growth phase, ensuring a normal distribution of cells in their various cell cycles. After cells have been detached from the culture flask, they were collected in 15 ml tubes, centrifuged at 1500 rpm and the supernatant was removed, the cells were gently rinsed with a phosphate buffered solution (PBS), re-centrifuged at 1500 rpm and that supernatant was again removed. The FSaII cells were then resuspended in regular media containing Gibco's Rapid Prototyping & Manufacturing Institute medium (RPMI-1640), and supplemented with 10% fetal bovine serum (FBS) (PAA Laboratories, Inc., Etobicoke, Ontario), penicillin (50 U/ml), and streptomycin (50 µg/ml) – fetal bovine serum (FBS), a nutrient source, served here to neutralize the activity of trypsin. The cellular concentration in suspension was then determined using a hemocytometer. Known numbers of cells were then seeded on flasks and allowed to rest, giving time for the newly transplanted cells to adhere to the flask and resume its normal functions. This time

is typically 14-16 hours between seeding cells and irradiation, because enough time should be given for the cells to attach and resume its normal functions, but not so much time that cells begin dividing and as such increasing the number for cells being treated to an unknown number. For this experiment, the cells were irradiated using the Philips RT-250 Orthovoltage external beam x-ray machine at 250 kVp (Philips Medical System, Brookfield, WI), with added filtration of 1.0 mm Al and 0.35 mm Cu for the low energy x-rays, delivering at a dose-rate of approximately 1 Gy/minute. Various increasing doses of radiation were delivered in a single fraction, while having one group of flasks set aside to receive a 0 Gy dose, as the control group. The purpose of including controls is to determine what is known as the plating efficiency (PE). After irradiations, all cells were returned to an incubator for about 7-10 days. The colonies formed were rinsed with phosphate buffered saline, fixed with a mixture of methanol and acetic acid (10:1 v/v), stained (using 0.5% crystal violet and 25% methanol solution), rinsed in water, then allowed to dry in an oven overnight. Colonies with more than 50 cells were counted. An example of the stained colonies can be seen in Figure 1.2.d.

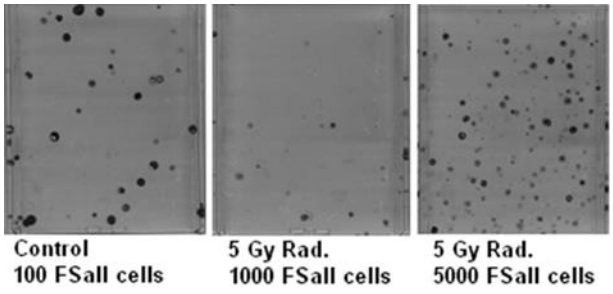

Figure 1.2.d Image of stained macroscopically visible colonies of FSaII cells. The control flask was seeded with 100 cells while the radiation treated flasks were seeded with 1000 and 5000 FSaII cells respectively.

The plating efficiency of control cells was used to normalize the surviving fraction of irradiated cells.

$$Plating\ Efficiency\ (PE)\ =\ \frac{Number\ of\ colonies\ observed}{Number\ of\ cells\ seeded}$$

Next the surviving fraction (SF) is determined for all the treated groups, which is the number of colonies counted divided by the plating efficiency normalized number of cells seeded.

$$Normalized\ Surviving\ Fraction\ (SF)$$

$$= \frac{Number\ of\ colonies\ counted}{Number\ of\ cells\ seeded\ \times (PE/100)}$$

The resulting survival fraction of FSaII cells exposed to x-rays can be seen in Figure 2.2.e (section A), where the SF is plotted on a log scale on the y-axis and the radiation dose is linearly plotted on the x-axis.

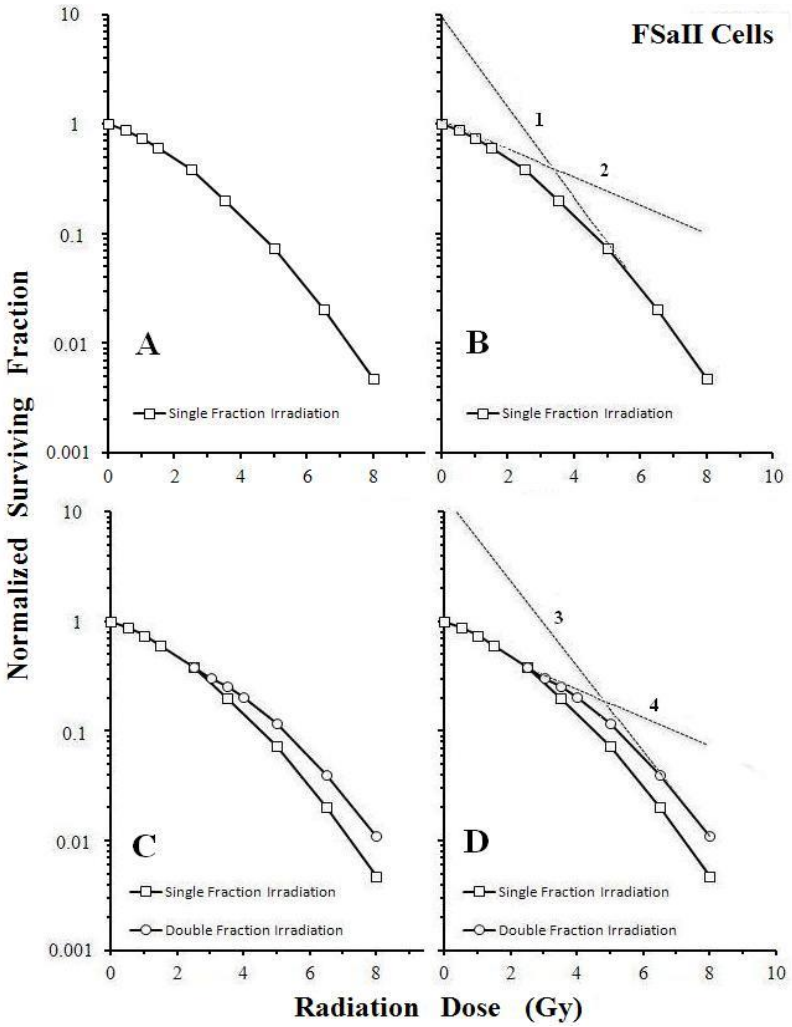

Figure 2.2.e Survival curve of FSaII cells to various doses of x-rays. Section A depicts the survival of FSaII cells after various integral doses of radiation in a single fraction. Section B highlights the characteristic biphasic nature of the survival slope in section A with its extrapolation lines. Section C depicts the resulting survival curve when the radiation dose greater than 2.5 Gy is split into two fractions where the first fraction is 2.5 and the second fraction being the difference between the first 2.5 Gy and the intended total dose. The second slope indicates that splitting dose increases the cell's ability to survive. Section D indicates the biphasic nature of the second fractionated curve, and its similarity in slope to the original single fraction curve.

According to the single ionizing event of a single target theory that was modeled with Poisson's statistics, we expected only one straight line. However as can be seen by this curve, it is bi- phasic, meaning it is comprised of two different exponential functions which are extrapolated in section B, one exponential function representing the lower radiation doses {2} and the other representing the higher radiation doses {1}. The bi-phasic curve therefore infers both a single ionizing event and multiple targets situation and multiple ionizing events for each target. In the first instance the equation, $SF = e^{-\alpha D}$, satisfies the case where a single ionizing event with multiple targets causes the loss of clonogenic potential while the equation, $SF = e^{-\beta D^2}$, satisfies the case where multiple ionizing events with a single target causes the loss of clonogenic potential, with 'β' representing the slope of that curve while the dose is squared. The combination of these two models is known as the linear-quadratic model.

$$SF_{\text{whole curve}} = e^{-\alpha D-\beta D^2}$$

Given that the 'target' of interest is DNA, when there is a loss of clonogenic potential, what is being referred to is the literal breaks or aberration in the chromosome due to radiation induced ionizations. In order to decrease the clonogenic potential of a cell, irradiation needs to produce double strand breakage (14) (15). In the case where a single ionizing event with multiple targets causes the loss of clonogenic potential, it refers to one ionizing event leading to a double strand break, and in the case where multiple ionizing events act on a single target, it also refers to a double strand break with contributions from independent ionizing events.

2 Anti-Cancer Properties of Experimental Drug β–Lapachone

2.1 β–Lapachone's Cytotoxicity

β–Lapachone is a quinone-like compound found in the bark of the Lapachone trees (Figure A2), which are native to central south America, and have been used for hundreds of years for its medicinal qualities, including but not limited to anti-bacterial, slowing age related degeneration and amelioration of obesity and related phenotypes in mice (55) (56). Importantly, β–Lapachone has recently been found to poses strong anti-cancer properties. β–Lapachone's anti-cancer properties stem from the fact that it is 'bio-activated' inside the cell by the enzyme NQO1 and its cytotoxicity is a result of several contributing factors, namely β–Lapachone's unique ability to generate reactive oxygen species. When β–Lapachone in its quinone form (β–Lap Q) enters cells, it is activated by the engyme NQO1 which reduces β–Lap Q with two electrons to β–Lapachone hydroquinone (β–Lap HQ) using NADH or NADPH as electron sources. However, β–Lap HQ is an unstable molecule and spontaneously oxidizes back into its original β–Lap Q form. If β–Lap HQ oxidizes back to β–Lap Q one electron at a time, as opposed two electrons oxidization in a single step, there will be an intermediary form known as β–Lapachone semiquinone (β–Lap SQ) is formed. When β–Lap HQ oxidizes via β–Lap SQ in the presents of cytosolic oxygen [O_2], superoxides [O_{2-}] and in turn hydrogen peroxides [H_2O_2] are formed.

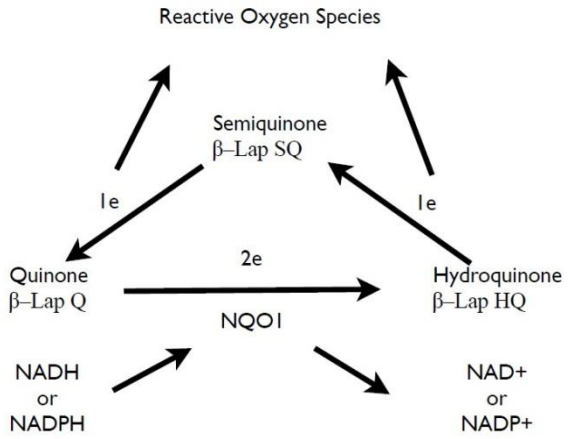

Figure 2.1.a. Flow diagram showing NQO1 reducing β–Lapachone in the quinone form (β–Lap Q) to β–Lapachone in the hydroquinone form (β– Lap HQ) by use of NADH or NADPH electron donation. β–Lap HQ is unstable and under goes a single electron oxidation to a β–Lapachone semiquinone β–Lap SQ intermediary. When β–Lap HQ oxidizes back to β–Lap Q via β–Lap SQ in the presence of cytosolic oxygen, superoxides and hydrogen peroxide are generated.

When β–Lapachone is oxidized back into its original quinone form, it is again available to be reduced by NQO1. As can be seen in Fig 2.1.a, β–Lapachone's changes from its quinone form to its hydroquinone from and back again to its quinone form, sometimes via its semiquinone form, and as such a futile cycling is initiated. It is this futile cycling that is responsible for β–Lapachone's cytotoxicity. It is proposed that this futile cycling severely depletes intra-cellular NADH and NADPH, which in turn depletes adenosine triphosphate (ATP) leading to increases in cytosolic Ca^{2+} released from the endoplasmic reticulum. Increased Ca^{2+} in the cytosol causes depolarization of the mitochondrial membrane leading to pore formation and release of sequestered cytochrome C which in turn leads to the activation of caspase 9 and the

induction of apoptosis (57) (58). In conclusion, the cytotoxic effect of β–Lapachone stems from two mechanisms: formation of ROS and depletion of NADH and NADPH. β–Lapachone's cytotoxicity can be measured in vitro by determining its clonogenic surviving potential. In order to determine the cytotoxicity of β–Lapachone, an in vitro experiment was set up using two different cell lines, concentrations of β–Lapachone and time for the cells to be exposed to it.

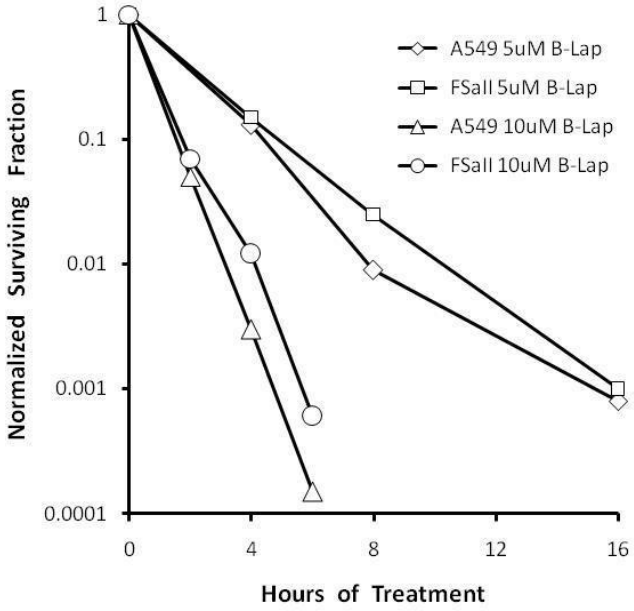

Figure 2.1.b. Clonogenic survival curve of FSaII and A549 cells exposed to β–Lapachone for different lengths of time at 5 and 10 µM. The Standard Error (which is smaller than the points) was calculated by dividing the sample standard deviation and the square-root of the number of experiments representing each data point. Source: Compiled experimental data from the Radiation Biology Laboratory at the University of Minnesota.

Based on this result, the following pertinent conclusions can be drawn:

1. β–Lapachone's cytotoxicity increases with exposure time to the cell, and so is time dependant.
2. β–Lapachone's cytotoxicity increases with its concentration, and so is not phase specific in vitro.

2.2 NAD(P)H: quinone oxidoreductase 1 (NQO1)

The NQO1 has been shown to be a detoxifying enzyme according to several studies (39) (44) (45) (46) (47). NQO1 is a cytosolic reductase which uses NADH or NADPH as an electron source (48) to reduce quinones to hydroquinones in a single two-electron step, as can be seen in the flow diagram in Figure 2.2.a.

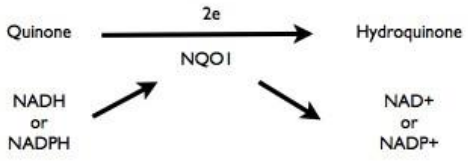

Figure 2.2.a. Flow diagram showing normal NQO1 activity – reducing a quinone to a hydroquinone by use of NADH or NADPH electron donation.

NQO1 concentration is high in cells requiring antioxidant protection, such as lung epithelial, breast and colon, and vascular epithelium to name a few (44) (49). Interestingly, many cancer cells also over-express NQO1, which opens the possibility for NQO1 mediated anti-cancer therapies (50) (51) (52). It has been shown that the levels of cytosolic NQO1 can be further up-regulated through various cell stressing mechanisms,

including treatments involving cisplatin, mild heating (mild-temperature hyperthermia) and ionizing radiation (53) (54).

The purpose of this project was to understand how therapeutically relevant doses of ionizing radiation can influence NQO1 intracellular levels. In order to observe possible post- irradiation changes in the intra-cellular levels of NQO1, a protein immunoblot analysis was done on the A549 cells (human non-small-cell lung adenocarcinoma) at various time points after an exposure to 4 Gy in a single fraction. Below is a schematic representation of the major steps for a typical protein immunoblot assay.

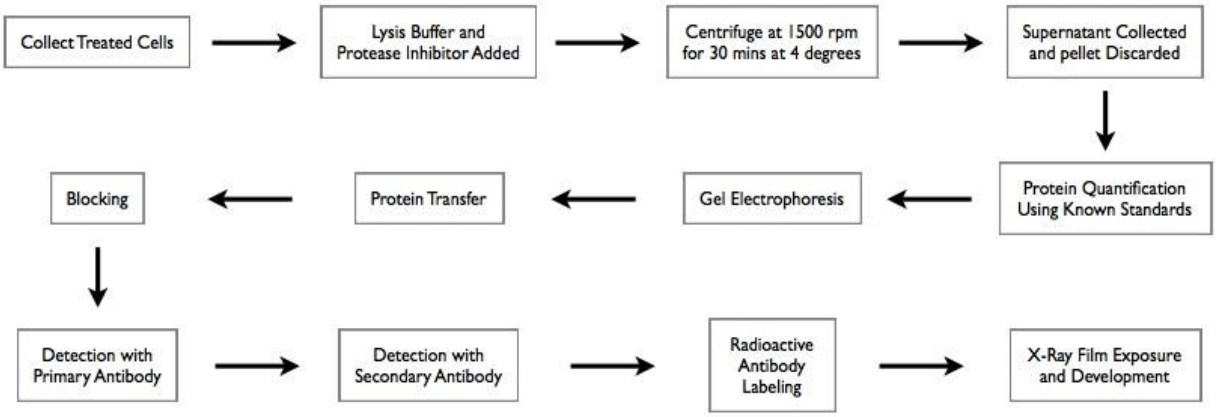

Figure 2.2.b. Flow diagram showing the main steps of the protein immunoblot assay.

Experimental Determination of Changes to Intra-Cellular NQO1 Levels in Irradiated Cells

A549 cells growing exponentially in vitro were harvested, using 0.25% of a digestive enzyme solution, trypsin, containing ethylenediaminetetraacetic acid (EDTA) for 5 minutes at 37ºC were used. After cells have been detached from the culture flask, they were collected in 15 ml tubes, centrifuged at 1500 rpm and the supernatant was

removed. The cells were then gently rinsed with a phosphate buffered solution (PBS), re-centrifuged at 1500 rpm and that supernatant was again removed. The A549 cells were then resuspended in RPMI-1640 medium, and supplemented with 10% fetal bovine serum (FBS) (PAA Laboratories, Inc., Etobicoke, Ontario), penicillin (50 U/ml), and streptomycin (50 µg/ml). Fetal bovine serum (FBS), in addition to supplementing cellular nutrition, also serves to neutralize the activity of trypsin. The cellular concentration in suspension was then determined using a hemocytometer. Cells were then seeded on new growing flasks and allowed to rest, giving time for them to adhere to the flask and resume its normal functions. This time is typically 14-16 hours between seeding cells and irradiation, because enough time should be given for the cells to attach and resume its normal functions, but not so much time that cells begin dividing and as such increasing the number for cells being treated to an unknown number. After cells were exposed to 4 Gy irradiation, they were returned to the incubator for: 0h (control), 2h, 4h, 8h, 12h, 24h, 48h, 72h and 96h. When the end time points were reached, cells were removed from the incubator, rinsed twice with phosphate buffered solution (PBS), trypsinized with 0.25% trypsin solution containing ethylenediaminetetraacetic acid (EDTA) for 5 minutes at room temperature. The detached cells were collected in 15 ml tubes, centrifuged at 1500 rpm for 5 minutes and the supernatent was removed gently rinsed again with PBS, re-centrifuged and that supernatent was again removed. The cells, now collected into a pellet, were lysed with 100 µl of lysis buffer while 15 µl of protease inhibitor was added to protect cytosilic enzymes from being cleaved by proteasomes. The lysed cells were then kept at - 80 ºC until all the cells from each end-time point has been collected. The frozen (-80 ºC) cells were put on ice to slowly thaw, gently vortexed, and centrifuged at 4

ºC (in a cold room) at 14,000 rpm for 20 minutes. The NQO1 containing supernatant was then collected and transferred into respective tubes in preparation for a bicinchoninic acid (BCA) based general protein concentration analysis using protein standards for a protein concentration reference. For the BCA analysis, a 96 well plate was used to hold three duplicates of each of the samples and three duplicates of each of the protein standards with the following solution for each well having a final volume of 229 µl containing: 200 µl of BCA solution – [1 gm sodium bicinchoninate, 2 gm sodium carbonate, 0.16 gm sodium tartrate, 0.4 gm NaOH, and 0.95 gm sodium bicarbonate, brought to 100 ml with distilled water and adjusted to pH 11.25 usuing 10 M NaOH] || 4 µl of cupric sulfate solution – [0.4 gm cupric sulfate (5x hydrated) in 10 ml distilled water] || 25 µl of protein sample solution – [88 µl of PBS and 12 µl of protein sample (supernatant)]. After all the samples were loaded into a 96 well plate, they were incubated for 30 minutes at 37 ºC. At the end of the incubation period, the plate was loaded onto a spectrophotometer and optical density was read at 562 nm. Optical densities of known protein concentrations were used to create a standard curve, as can be seen in Figure 2.2.c., against which the unknown protein concentrations of the experimental samples were determined.

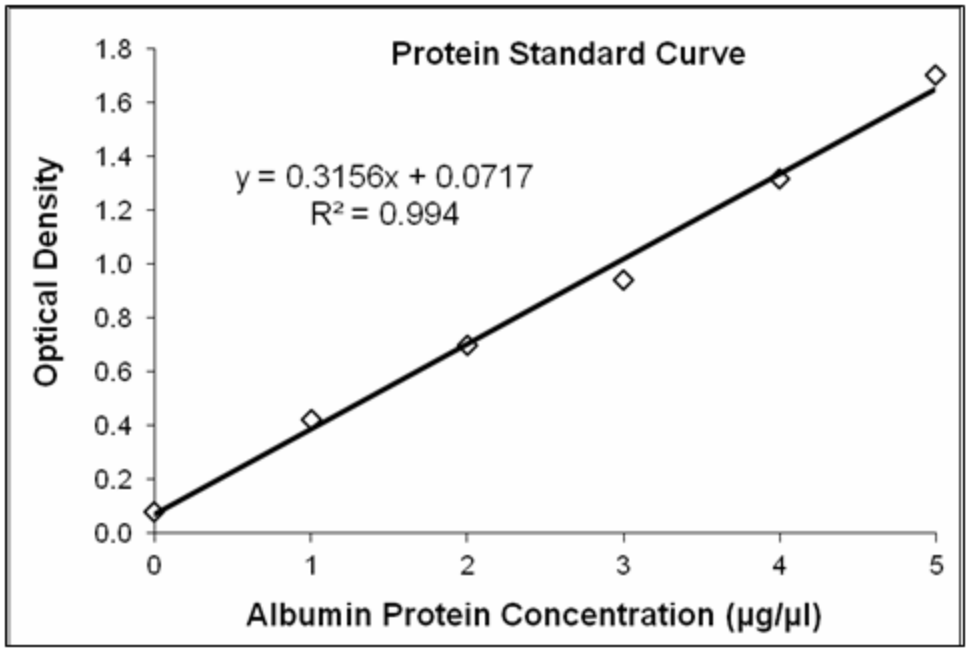

Figure 2.2.c. Protein standard curve showing the resulting optical density as measured by the spectrophotometer against the average of three protein samples of known concentrations after 30 minutes of incubation in a bicinchoninic acid solution. The R^2 coefficient of determination for this curve is 0.994, which is the statistical measure of how well the regression line approximates the real data points.

In order to isolate the protein of interest, NQO1, protein samples were analyzed using gel electrophoresis. This technique differentiates protein based on their electric charge, where the quantity of the electric charge directly correlates with the mass of that protein – the smaller the proteins mass directly corresponds to a smaller net charge. Smaller messes of protein travel furthest through the gel compared to larger protein for the same period of time. In order to prepare samples for gel electrophoresis, the protein concentration of the sample protein was determined from measurements using the protein standard curve. Based on previous protein immunoblot trial experiments with the NQO1

protein, a total protein concentration of 15 µg and total volume of 30 µl were selected to be loaded into the wells of the gel. The finial volume was determined by combining 15 µl of sample buffer with the remainder of the volume comprising the volume of sample protein needed to have 15 µg of protein and the remainder of the volume being lysis buffer. To this finial concentration, β-mercaptoethanol was added to reduce the protein disulfide bonds. The 30 µl final solutions were placed in microtubes and heated for 5 minutes at 100 ºC in a water bath. After the gels wells were carefully loaded – with the first well with 20 µl of rainbow protein marker, and the rest of the wells with the heated final solutions – the voltage was set to 50V for the first 30 minutes so that all protein containing samples entered the gel, and then switched to 100V for another 2 hours.

After running the gel electrophorese, the proteins were then dispersed within the gel in a protein mass dependent manner. In order to detect our specific protein, all the protein were carefully transferred from the running gel to a polyvinylidene difluoride (PVDF) membrane at 4ºC at 400 mA for 1 hour, a process known as 'blotting'. Membrane containing protein was washed in tris-buffered saline containing Tween-20 (TBST) and then blocked using 5% milk dissolved in TBST for 1 hour at room temperature on a gentle rocker. The blocking solution was then discarded and a new blocking solution was added containing a mouse derived anti-NQO1 primary anti-body (1ºAB), acquired from Abcam plc (Cambridge, England). Our desired dilution was 1:1000 1ºAB solution to blocking solution, or 1 µl of 1ºAB solution (1 µg/µl) in 1 ml, which would give a desired 1 µg/ml for a final concentration. 1ºAB solution was left rocking gently with the protein PVDF membrane overnight at 4 ºC. On the next morning, the 1ºAB was removed and the membrane was rinsed three times with TBST for 15 minutes each time at room

temperature on a rocker. Next, the membrane was blocked in a similar manner for 1 hour followed by adding transferring the membrane into a secondary anti-mouse alkaline phosphatase linked (AP) antibody (2ºAB-AP) solution for another hour. The 2ºAB-AP solution was diluted to 1:2000 2ºAB-AP solution to blocking solution, or 1 µl of 2ºAB solution (1 µg/µl) in 2 ml, which would give a desired 0.5 µg/ml for a final concentration. After 1 hour of incubation at room temperature on a rocker, the membrane was rinsed three times for 15 minutes each time with TBST. The membrane was allowed to dry and exposed to an electro-chemi-fluroluminescent substrate (ECF) for 4 minutes before scanning. The ECF caused the alkaline phosphatase attached to the anti-mouse antibody to florescent in the blue spectrum. Fluorescing membrane was imaged using the photometer Storm 860 Scanner.

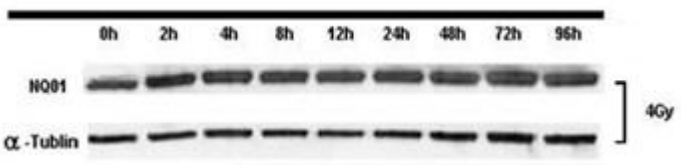

Figure 2.2.d. Film exposure showing relative levels of NQO1 in A549 cells. The 0h group without radiation (control) and post-irradiation of 4 Gy at the following post-irradiation times: 2h, 4h, 8h, 12h, 24h, 48h, 72h and 96h. Also shown are levels of alpha-tublin for each sample.

As can be seen in Figure 2.2.d., levels of NQO1 began to rise as early as 4 hours post irradiation and reached a maximum at about 24 hours and remains elevated for more than 72 hours later when compared to the un-irradiated cells. Based on this result, the following conclusions can be drawn:

3. Levels of NQO1 are up-regulated by ionizing radiation of 4 Gy.

4. Levels of NQO1 remains at elevated for more than 72 hours after 4 Gy.

3 Radiation and β–Lapachone Synergism

The combination of therapeutically relevant radiation treatments and β–Lapachone treatments shows that there is biologically measurable interaction between the two, in that each treatment modality complimentary potentiates the cellular lethality of the other.

3.1 Complimentary Potentiating Mechanisms

As has been previously discussed, radiation and other cell stressing modalities (59) up- regulates the concentrations of NQO1 enzyme, which may lead to cell death. However, in addition to this mechanism, it has been observed, and described below, that β–Lapachone enhances the sensitivity of cells to radiation. The following is a description of β–Lapachone's radiation sensitizing effects.

A549 and FsaII cell lines were used to access the effect of combined radiation and β–Lapachone treatments on cancer cells in vitro. The aim of this study was to determine whether β–Lapachone increases A549 cells sensitivity to radiation. In preparation, the cells were gently harvested, counted and appropriately plated into t-25 flasks in duplicates of three for each data point, from a healthy exponentially growing stock. Cells were plated for three treatment groups: 'Radiation only' group where cells were irradiated in single fraction, 'Drug only' group that was further split into two sub groups each receiving different concentrations of β–Lapachone, and the 'Combined radiation and drug group' for each radiation dose point. In the radiation only group, the dose point of 0 Gy

served as a global control for plating efficiency, the drug only group served as a control for the combined treated group, for the respective β–Lapachone concentration. β–Lapachone concentrations of 5 µM and 2.5 µM were prepared by adding 2.423 grams to 10 ml of supplemented media to make a 1 mole stock – 15 µl of the stock solution was added to 3 ml of supplemented media to make the working solution of 5 µM – some of the 5 µM working solution was diluted with supplemented media by a factor of 2 to get the working solution of 2.5 µM. Both the radiation only groups and the combined treated groups were irradiated with their respective doses in a single fraction. Immediately after irritation, combined treated groups and drug only groups were treated with β–Lapachone for 2 hours at their respective concentrations in an incubator, then all groups were gently rinsed with phosphate buffered saline (PBS) twice before adding supplemented media and returning them to an incubator for about 7- 10 days or until there are colonies visible to the eye. At this point, colonies were rinsed with sterile saline, fixed with a mixture of methanol and acetic acid (10:1 v/v), and stained using 0.5% crystal violet solution in 25% methanol for another 10 minutes, rinsed in water, then allowed them to dry in an oven overnight. Colonies containing more than 50 cells were counted. The average of the triplicate for each data point was determined and divided by the number of cells plated for that respective data point, for determination of the fractional survival of the cells. The normalized survival was determined by dividing the fractional survival of that data point by the fractional survival of the 0 Gy control; the normalized survival of the global control is consequently 1. Next, the combined treated group was normalized for the toxic effects of β-Lapachone action only by dividing the fractional survival of the combined treated groups by their respective drug concentrations of the fractional survival of the

drug only group.

$$\text{Drug Normalized Survival Combined Treated Group} = \frac{\text{Fractional Survival of Combined Treated Group}}{\text{Fractional Survival of Drug Only Group}}$$

This data was then plotted and can be seen in Figure 3.1.a.

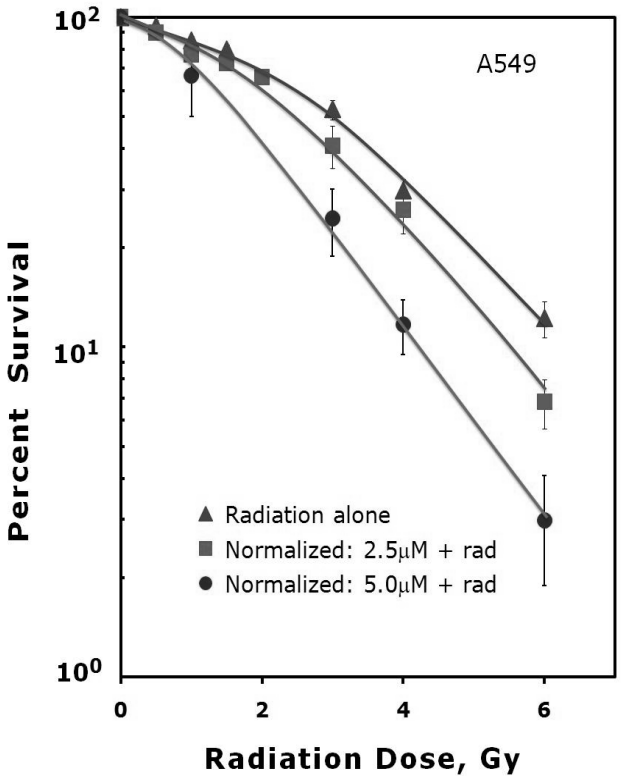

Figure 3.1.a. A549 cells treated with radiation alone or in combination with β–Lapachone. A characteristic radiation survival curve is shown for cells receiving only radiation, while cells that were treated with β–Lapachone for 2 hours immediately after irradiation shows a marked increase in sensitivity. An increase in sensitivity to the effects of radiation can be observed in correlation with an increase in β–Lapachone's concentration from 2.5 μM to 5 μM.

As can be seen, the normalized combined treated groups showed increased radiation sensitivity by β–Lapachone in a drug concentration dependent manner. In order to better understand how the cells became sensitive to radiation, it is important to understand the possible effects β–Lapachone may have on the cell's normal ability to repair itself after radiation- induced ionizing stress to the DNA; specifically, of interest is whether β–Lapachone sensitizes cells to radiation by suppressing 'sub-lethal damage' repair.

Sublethal damage repair is the operational term that describes increase in cell survival when a given radiation dose is split into two (or more) parts by a time interval. A dose of radiation lethal to a cell when delivered in a single fraction may not be lethal if the radiation dose is split into two fractions separated by a certain period of time; because some of the damage to the DNA is repaired during the time between radiation exposures. The splitting of a radiation dose is called fractionation; the greater the amount of time between fractions, the more the damaged DNA is repaired up to a threshold where any additional time given for repairs would not increase the odds of survival. After radiation exposure, various cell cycle checkpoint genes are activated, which brings about cell cycle arrest – allowing time for the repair of damaged DNA. If the inter-fraction time is sufficiently long, damage repair continue through the cell cycle checkpoints. Experimentally, the extent of sublethal damage repair can be quantified. The ratio of the number of surviving cells, resulting from the fractionated dose can be compared to the number of surviving cells, resulting from the same dose given in a single fraction. This is called the recovery factor. In vivo experiments show a clear suppression of sublethal damage repair for hypoxic tumors (18). This is clinically relevant because the cancer cells

comprising a tumor become hypoxic at only 70-80 μm away from blood vessels in part due to the diffusion limit of oxygen and the very high metabolism of each cancer cell. However it is important to note that hypoxic cells have an increased ability to survive a single fraction of radiation dose in comparison to a normoxic cell. The ratio of doses necessary to produce the same level of cell killing under hypoxic to aerated conditions is called the oxygen enhancement ratio.

In order to address the question of whether β–Lapachone sensitizes cells to radiation by suppressing 'sublethal damage' repair, FSaII cells were divided into four groups as follows: 'Radiation only' group where cells were irradiated in single fraction, 'Fractionated radiation only' group where cells were irradiated in two fractions with 2 hours separating the two fractions, 'Drug only' group receiving 2.5 μM of β-Lapachone for 2 hours, and the 'Combined fractionated radiation and drug group' where cells were treated with β–Lapachone for two hours following the second fraction of radiation. In the radiation only group, the dose point of 0 Gy served as a global control for plating efficiency, the drug only group served as a control for the combined fractionated radiation and drug group.

The radiation only group was irradiated with various doses in a single fraction. The fractionated radiation only group and combined fractionated radiation and drug group also received its first fraction of radiation at this time, starting at the 2.5 Gy dose point, for all total dose end points. All cells of both the fractionated radiation only group and the combined fractionated radiation and drug groups were returned to the incubator for the 2 hours inter- fraction time. After 2 hours, both the fractionated radiation only group and the combined fractionated radiation and drug groups received the second

fraction of radiation; the dose of the second fraction was determined by subtracting 2.5 Gy of the first fraction from the total intended dose. The drug only and combined fractionated radiation and drug groups were then treated with
2.5 μM of β–Lapachone for 2 hours and returned to an incubator. After 2 hours of β–Lapachone treatment, all four groups were gently rinsed with phosphate buffered saline (PBS) twice before adding normal supplemented media and incubated for 7-10 days. Colonies were rinsed with sterile saline, fixed with a mixture of methanol and acetic acid (10:1 v/v), stained, rinsed in water, and then allowed to dry in an oven overnight. Colonies comprising more than 50 cells were counted. The normalized survival and the drug normalized combined treated group were determined and described in similar manner above, and are graphically represented in Figure 3.1.b below.

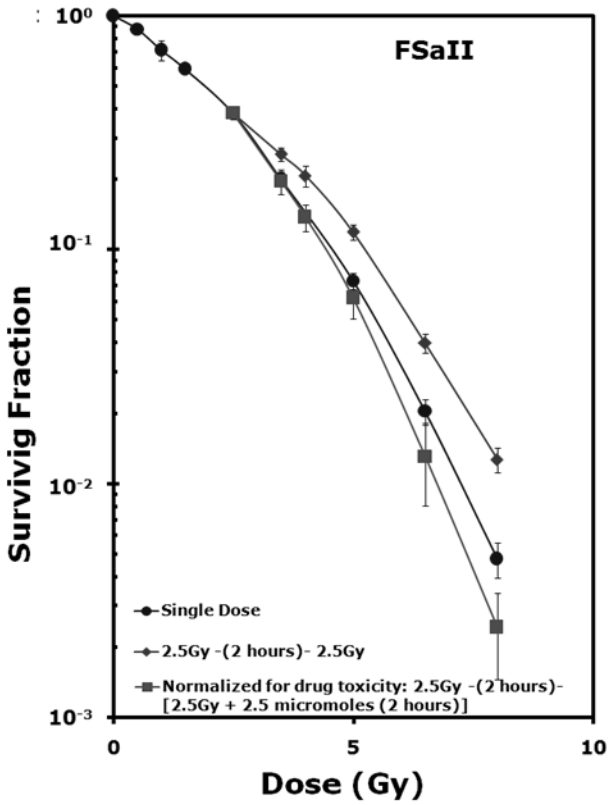

Figure 3.1.b. Survival of FSaII cells after various doses of radiation in one or two fractions. A characteristic radiation survival curve is shown for cells receiving only radiation, while cells that were treated with β–Lapachone for 2 hours immediately after a second fraction of irradiation shows a marked increase in sensitivity even after normalizing for the effect of β–Lapachone alone due to suppression of SLD repair. All cells received a total of one fraction for doses 2.5 Gy and lower, while doses larger than 2.5 Gy received a total of two radiation doses where the first dose totaling 2.5 Gy and the second dose being the difference needed to achieve the intended total dose. Cells receiving 2.5 μM of β–Lapachone were drugged for 2 hours following the second fraction of radiation.

As can be seen in Figure 3.1.b, the survival curve of cells receiving radiation only in a single fraction shows a D_0 value of 2 Gy. In the survival curve of cells receiving two exposures of radiation, a clear survival increase can be observed over the single fraction radiation only curve, indicating a sublethal damage repair. The combined treated group where cells were irradiated identically to the split dose radiation only group, and were then treated with 2.5 μM of β–Lapachone for 2 hours, were normalized for the independent influence on these cells from the 2.5 μM of β–Lapachone for 2 hours alone, and plotted. The survival curve, of cells treated with both 2.5 μM of β–Lapachone and two exposures of radiation, showed significant cell lethality when compared to its counterpart, the split dose radiation only curve. Additionally, this combined treated group showed a lower survival than that of the single fraction radiation only curve. This suggest that not only was there suppression of sublethal damage repair with a nominal treatment of β–Lapachone after the second fraction of radiation, but there even was increased

sensitivity beyond the suppression of repair as indicated by the fact that the combined curve was steeper than that of the radiation only single fraction curve. In further analysis of the effects of β–Lapachone's sublethal damage repair suppression, the fractionated radiation dose was held constant while varying the inter-fraction time from 1 - 5 hours, in the presents of 2.5 μM of β–Lapachone during the entire inter-fraction time. Three groups were set-up as follows: 'Fractionated radiation only' group, where cells were irradiated in two equal fractions with a total dose of 5 Gy, 'Drug only' group receiving 2.5 μM of β–Lapachone for the entire inter-fraction period, and the 'Combined fractionated radiation and drug group' where cells were drug treated for the entire inter-fraction time following the first fraction of radiation. In the radiation only group, the dose point of 0 Gy served as a control for plating efficiency, the 5 Gy dose point served as the point at which fractionated survival is compared, and the drug only group served as a control for the combined fractionated radiation and drug group. For this experiment, cells and β–Lapachone concentration of 2.5 μM were prepared similarly to the previous experiment. On the day of treatment, the fractionated radiation only group and the combined fractionated radiation and drug group were irradiated at 2.5 Gy for the first fraction. The combined fractionated radiation and drug group and the drug only group were then treated with a β–Lapachone solution of 2.5 μM for the duration of the inter-fractionated period of 1 – 5 hours at 1 hour increments. All cells were then returned to the incubator for their respective inter-fraction time. After the inter-fraction time was completed, both the fractionated radiation only group and the combined fractionated radiation and drug groups received the second fraction of radiation, gently rinsed with phosphate buffered saline (PBS) twice, and cultured in regular media for about 7-10 days or until there are

colonies visible to the eye. Colonies were rinsed with sterile saline, fixed with a mixture of methanol and acetic acid (10:1 v/v), and stained using 0.5% crystal violet solution in 25% methanol for another 10 minutes, rinsed in water, then allowed to dry in an oven overnight. Colonies comprising more than 50 cells were counted. After all data for the treatment groups were normalized for plating efficiency, and the combined treated group was normalized for each respective drug only, the recovery factor was determined by comparing the normalized survival of all dose points receiving fractionated irradiation to the survival of cells receiving a single fraction dose (of 5 Gy).

$$\text{Recovery Factor} = \frac{\text{Normalized Survival of Data Point}}{\text{Normalized Survival of Single Fraction Data Point}}$$

This experiment was repeated 6 times and was again repeated 7 times using the A549 cell line, where A549 cells received a total dose of 6 Gy, split into two equal fractions and FSaII cells received a total of 5 Gy split into two equal fractions. The recovery factor for fractionated radiation only group and the drug normalized combined fractionated radiation and drug group were determined and graphically represented in Figure 3.1.c below.

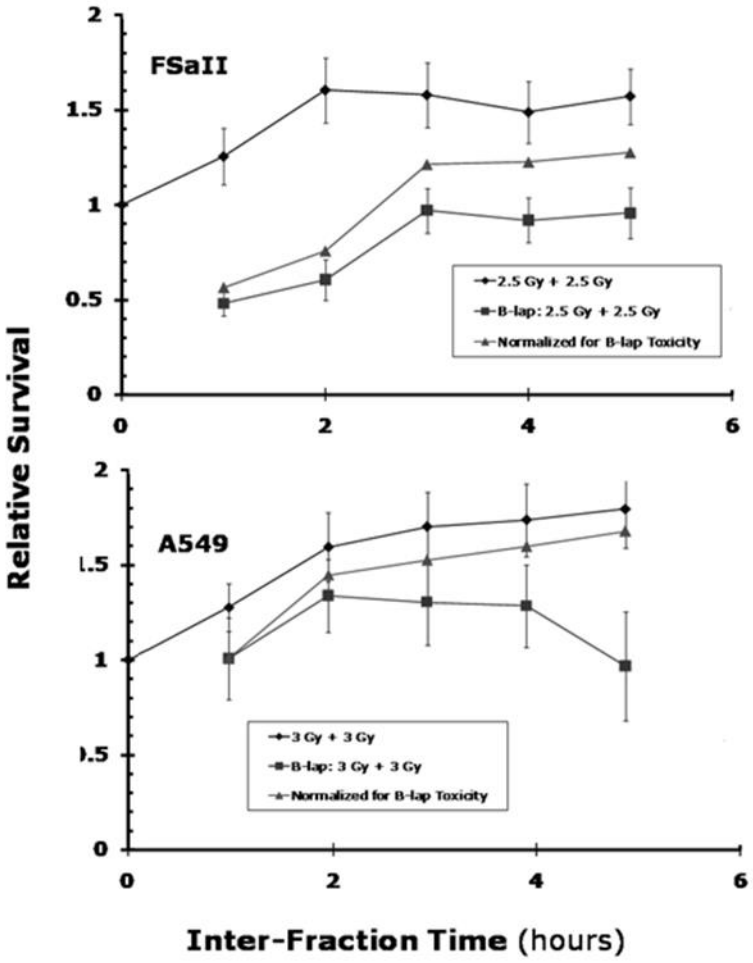

Figure 3.1.c. FSaII and A549 cells were irradiated with 5 Gy and 6 Gy respectively in a single dose or in two equal doses (2.5 Gy + 2.5 Gy) and (3 Gy + 3 Gy) respectively, separated by different time intervals in the absence or presence of 2.5 μM β–Lapachone. The survival of FSaII cells irradiated with 5.0 Gy given in two doses of 2.5 Gy progressively increased as the time interval between the two doses was increased up to 2 hours, demonstrating the sublethal damage caused by the first 2.5 Gy irradiation was repaired within 2 hours. When cells were maintained in 2.5 μM β–Lapachone, the split-dose effect was markedly suppressed. The combine effect was normalized for the cytotoxicity of 2.5 μM β–Lapachone. A549 shows similar results. These findings demonstrated that β–

Lapachone significantly suppressed the repair of sublethal radiation damage.

As can be seen in both FsaII and A549, the single fraction dose has a recovery factor of 1. As expected for recovery factor curves, the first 2 hours are the most critical period in which the majority of cells with sublethal DNA damages do most of its necessary repairs, after which point, allowing the cells additional repair time would only very modestly increase its viability. In both cases, the recovery has been suppressed even after accounting for the independent cytotoxic activities of β–Lapachone alone; consequently indicating suppression of the cell's ability to repair radiation induced sublethal damage to its DNA. Upon closer examination, the dose point at 5 Gy for the Figure 3.1.b, and the 2 hour inter-fraction time on Figure 3.1.b for the FsaII curve on appearance received very similar treatments, in that for both the fractionated radiation treatments, inter-fraction time, drug time and the drug concentration were identical, however, the drug treatment occurred after the first fraction of radiation in Figure 3.1.c and in Figure 3.1.b, the drug treatment occurred after the second fraction of radiation. In both cases, the drug normalized fractionated radiation (2.5 Gy – 2 hours – 2.5 Gy) cells had a lower survival that the single fraction radiation only (5 Gy), and much lower survival than the fractionated radiation only cells. Additionally, a marginal decrease in the cell's viability could be observed for the cells treated with β–Lapachone during the inter-fraction period as opposed to those that were treated after the second fraction, based on direct comparison at this dose point; consequently, suppression by β–Lapachone on the sublethal damage incurred by the first fraction of radiation is more effective than the suppression by β–Lapachone on the sublethal damage incurred by the first fraction of

radiation. In both cell lines however, it is clearly observed that even in the drug normalized combined treated groups, the cell viability increased with increased inter-fraction time suggesting other mechanisms at play. In the recovery of the combined groups there are competing mechanisms influencing the viability of the cells, the cell's natural ability to repair radiation induced sublethal DNA damage – which increases survival – and the cytotoxicity of β–Lapachone – which decreases survival. In the first two hours after the first fraction of radiation and β–Lapachone treatment, both mechanisms compete and influence the cell's viability, however, after 2 hours, the effects of sublethal damage repair significantly decreases while the cytotoxicity of β–Lapachone continually increases due to the complimentary action of radiation's up-regulation of activating enzyme, NQO1; therefore accounting for the relatively high drug normalized recovery factor of this group for inter fraction times greater than 2 hours.

Based on these results, the following conclusions can be drawn:

5. There is significant suppression of sublethal damage repair with a nominal treatment of β–Lapachone after the second fraction of radiation; moreover, there is increased sensitivity beyond the suppression of repair, which suggests other cellular mechanisms at play.
6. Suppression of sublethal damage repair is more effective when β–Lapachone is administered following the first fraction of radiation as opposed to the second fraction of radiation, where β–Lapachone's concentration and treatment times are equal.

3.2 β–Lapachone's Influence on the Cell Cycle

Understandings of the cell cycle are very important objectives in cancer research. In this study, which will be described in detail, it shows that the A549 cell cycle is indeed altered when treated with β–Lapachone, irradiation and their various combinations. More importantly, it is experimentally shown that there are evident differences in the proportions of cells in the various parts of the cell cycle after treating with 7.5 μM of β–Lapachone only and 4 Gy of radiation only. Furthermore, the proportions of cells in the various parts of the cell cycle of those treated with both 7.5 μM of β–Lapachone and 4 Gy of radiation more closely resemble those that received 7.5 μM of β–Lapachone only, indicating β–Lapachone's influence over irradiation as it relates to the cell's ability to cycle through its phases.

Cell Line Investigated and its Normal Environment

The A549 (Human lung adenocarcinoma epithelial cell line) was used exclusively for these experiments and was originally acquired from the American Type Culture Collection (Manassas, VA).

Treatment and Collection

For each experiment, t-25 flasks, each containing 0.5 x 106 cells, were divided into four groups (Control, Radiation, Drug only, and Combination) where each group

contained one flask for each designated end time point: 6, 12, 24, 36 and 48 hours. The selected radiation and drug dose and drug treatment duration for the treated groups were chosen, based on numerous past experiments, because the expected number of surviving cells would be numerous enough for statistical significance (>10,000 cells after flow cytometric gating – discussed below) while having a cell lethality which is greater than 50 percent for each treated group. The Drug

only group received 7.5 µM of β–Lapachone and was left in the incubator for 1 hour after which it was gently rinsed twice with Dulbecco's Phosphate Buffered Saline (DPBS) before being returned to the incubator. The combination group first received 7.5 µM of β–Lapachone and was then immediately irradiated with 4 Gy in a single fraction and then returned to the incubator for 1 hour after which it was gently rinsed twice in DPBS before being returned to the incubator. The radiation only group received 4 Gy in a single fraction and then returned to the incubator. The radiation and control groups were also gently rinsed with DPBS in a similar fashion and time as the other two groups to preserve experimental homogeneity. At each end time point, attached and floating cells from the appropriate flasks were collected in 15 ml tubes using 0.25% Trypsin with EDTA, centrifuged, resuspended in DPBS, centrifuged again and the supernatant was removed leaving only the cell pellet. The pellet was resuspended in 3 ml of 70% -20°C Methanol by slowly adding the methanol to the cell pellet and stored at 4°C for as short a time period as experimentally possible so that all time points have been reached or up to a week.

Flow Cytometry and Data Analysis for Cell Cycle Determination

After all the pellets for each end time point were frozen, the pellets from each group were thawed and collected by centrifuging the tubes and aspirating out the 70% methanol solution. Each pellet was then washed with 500 µl of DPBS and transferred to a microtube, centrifuged and resuspended in 0.525 ml of RNase/PI solution (0.125 mg RNase, 25 µl Propidium Iodide,
0.5 ml DPBS). Cells were then left protected from light at room temperature for 30 minutes to incubate. Next, each cell sample was filtered with a 70 µm sieve to separate still attached cells and analyzed by the flow cytometer for the relative concentration of DNA in each cell. For each cell sample, gating was used to exclude cell doublets, necrotic cells and other debris, while the retained cells were used to determine the proportions of cells in either G1, S, G2 or A (cells in the M phase were included in G2). The cell cycle distributions were analytically determined using the Dean-Jet-Fox mathematical modeling algorithm contained in the flow cytometry analysis software FlowJo (Tree Star, Inc. OR), which assumes that the S-phase can be modeled by a second degree polynomial (flowjo.com/v762/en/ccmodels.html), while having the constraint that G2 needs to have twice as much DNA as G1. Those results were plotted as a histogram, as can be seen in Figure 3.2.a. The average of six experiments were used to determine the correlation coefficients between the combination group and each of the other three groups using a simple Pearson's Correlation; results of which can be seen in Table 3.2.c.

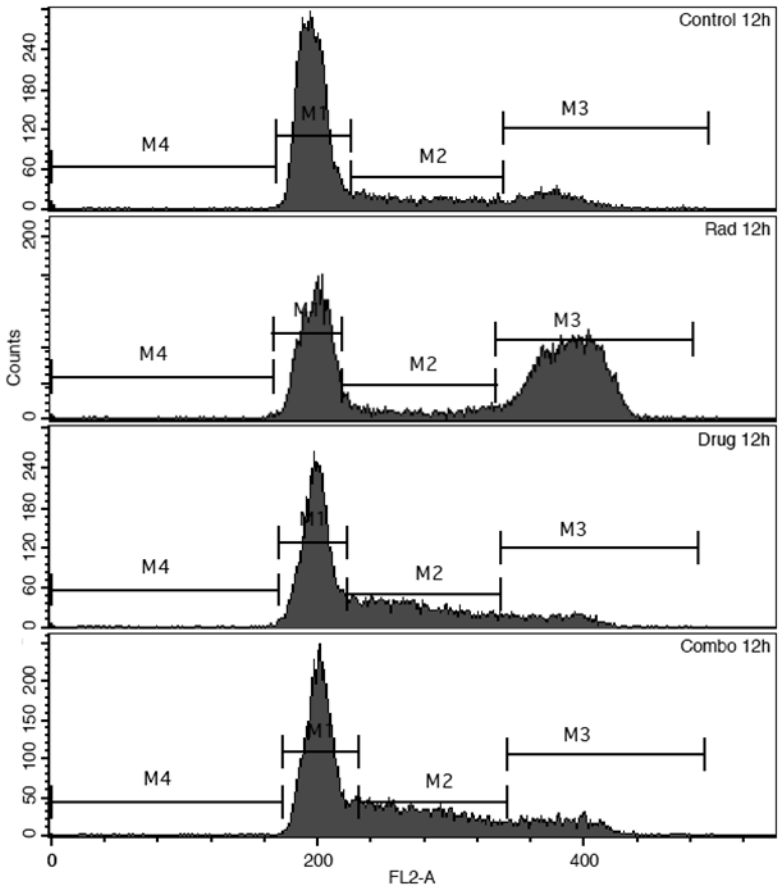

Figure 3.2.a. Histogram of the 10,000 cells within the gated portions of the total cell population for the four groups at the 12 hour post-treatment end time. Intensity of PI, which directly correlates with amount of DNA, is shown on the x-axis and the number of events (single intact cells) on the y-axis. M1, M2, M3 and M4 mark the approximate boundaries for G1, S, G2 and A cell phases respectively.

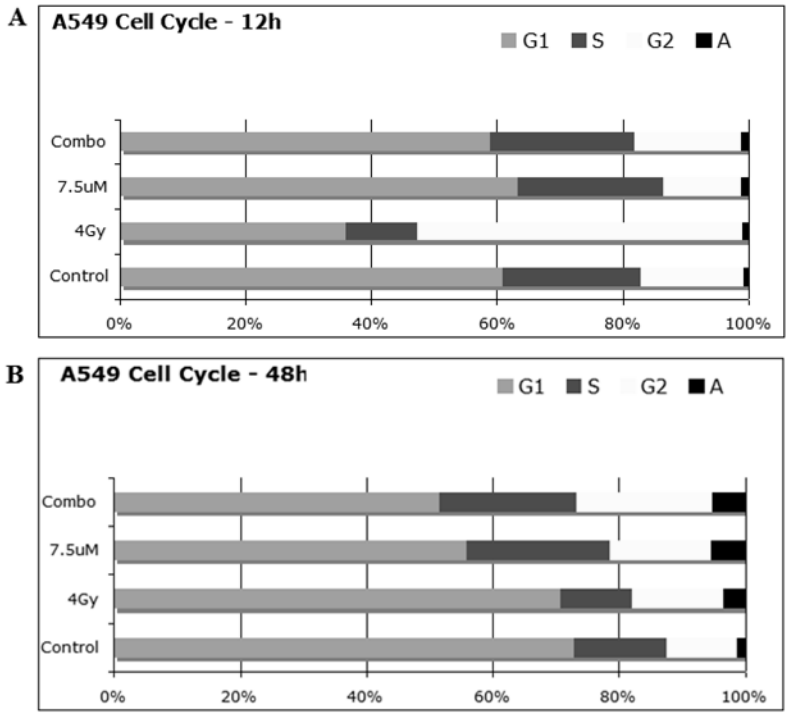

Figure 3.2.b. [A.] State of the cell cycle after 12 hours of treatment. At this time point, the correlation between the combination group and the radiation only group is the lowest for the 12 hour time point (r=0.4475). The correlation between the combination group and the drug only group is high (r=0.9953), as is the correlation between the combination group and the control (r=0.9995). [B.] State of the cell cycle after 48 hours of treatment. At this time point of 48h, the correlation between the combination group and the radiation only group is the highest for the 48h post-treated collection times (r=0.9633). However, the correlation between the combination group and the drug only group is even higher (r=0.9874), followed by the correlation between the combination group and the control (r=0.9688).

Pearson's Correlation Coefficient “r”

Post-Treatment End Time	Combined Treatment & Control	Combined Treatment & Drug	Combined Treatment & Radiation
6h	0.9946	**0.9994**	0.8207
12h	**0.9995**	0.9953	0.4475
24h	**0.9996**	0.9921	0.9713
36h	0.9969	**0.9990**	0.9718
48h	0.9688	**0.9874**	0.9633

Table 3.2.c. The Pearson's Correlation Coefficients between the proportion of cells in the various parts of the cell cycle, (G1, S, G2 and A) between the combination group and each of the other groups for each end time point. Numbers in bold and underlined shows the highest correlation for that end time point.

For all the post-treatment collection times, the proportions of cells in the various parts of the cell cycle, including apoptotic cells, for the combination group more closely followed those of the drug only group than those of the radiation only group. The following conclusions can be drawn from the results:

7. A population of A549 cells treated with 7.5 μM of β–Lapachone only modestly alters the proportions of cells in the various parts of the cell cycle, such as increased proportion of cells in the S-phase, when compared to untreated cells.
8. There is significant cell cycle arrest in A549 cells after irradiation of 4 Gy within the first 24 hours, however when cells are also under the influence of 7.5 μM of β–Lapachone, there is no discernible arrest in the cell cycle.

Given that Propidium Iodide was only used to quantify DNA content, pre-apoptotic cells would have been included in the G1, S, and G2 data shown in Figure 3.2.b in unknown proportions. Additionally, the flow cytometer calculates proportions based on the analysis of the first 10,000 gated events (which usually correspond to single cells), however it was observed that the pellet size of all β–Lapachone treated groups from 12 hours onwards were approximately half the size as those that did not receive β–Lapachone. This can be due to cell shrinkage or to cell degradation due to apoptosis, and as such the actual proportion of cells undergoing apoptosis cannot be stated with accuracy based on this study. To better understand the sensitivity of β–Lapachone and Radiation on each of the A549 cell cycle phase, a more accurate assessment of apoptosis was needed.

Determining Relative Pre-Apoptotic Activity for Each Cell Cycle Phase

In order to determine whether apoptosis occurred more often in certain parts of the cell cycle, the pre-apoptotic activities were measured along with the relative concentration of DNA. The caspases 3 and 7, which were used as the pre-apoptotic markers, were detected using a Fluorochrome-Labeled Inhibitors of the activated form of Caspases 3 and 7 (FLICA) reagent kit (Immunochemistry Technologies LLC, Bloomington MN). Caspases 3 and 7 were chosen because they are effector caspases, and their activated forms preclude the final steps in the apoptotic pathway where the cell dismantles the DNA and arrest general metabolic activity leading to the cell's death. The FLICA reagent is based on a membrane-permeable carboxyfluorescein linked peptide

sequence which only covalently binds to the activated caspases 3 and 7. FLICA freely diffuses across the cell wall and specifically binds to caspases 3 and 7 – upon washing; the unbound FLICA diffuses out of the cell so that the remaining bounded FLICA is a direct measure of the caspases 3 and 7 activity at the time of inoculation. The pellets of the treated cells were resuspended in 0.5 ml of serum free media containing 10 µl of FLICA working solution (50 µl DMSO + 200 µl PBS + FLICA reagent) and incubated for 1 hour while being protected from light. Cells were centrifuged and washed three times using phosphate buffered saline to rinse unbounded FLICA reagent, centrifuged and the supernatant was again carefully removed. Next the pellets were resuspended in 0.525 ml of RNase/PI solution (0.125 mg RNase, 25 µl Propidium Iodide, 0.5 ml DPBS) for DNA staining. Cells were incubated in dark for 30 minutes at room temperature. Next, each cell sample was filtered through a 70 µm sieve to separate attached cells and analyzed by the cytometer. Cells were not fixed after it was experimentally observed to reduce detection using the flow cytometer, and as such, special care was used to keep them cool while trying to minimize the overall time for labeling the cells. Untreated cells which did not receive either the FLICA reagent or DNA PI labeling [FL-PI-] were used as a double negative control in order to set the parameters for either keeping or excluding cells to be analyzed – specifically, electronically gating only whole intact single cells through the use of the forward and side scatter detectors, and as such exclude all the other detected events by the flow cytometer, as can be seen in Figure 3.2.d.

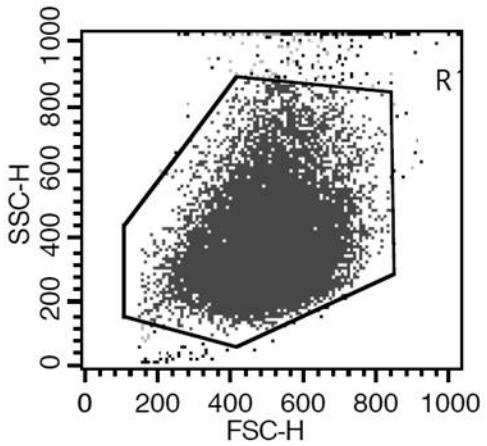

Figure 3.2.d. Gating of whole intact cells using the forward scatter channel (FSC-H) and side scatter channel (SSC-H) detectors.

In order to determine background levels of the pro-apoptotic markers caspases 3 and 7, untreated cells were prepared as described above with the FLICA reagent but without PI [FL+PI-]. Untreated cells were also used to determine background levels of the pro-apoptotic markers caspases 3 and 7 without using the FLICA reagent but with PI [FL-PI+]. Untreated cells receiving both the FLICA reagent and PI [FL+PI+], were used to determine the normal cell cycle distribution and the normal proportion of pre-apoptotic cells with active caspases 3 and 7 with-in each cycle. These untreated double positive controls were then compared with cells that were treated with 7.5 μM of β–Lapachone for 1 hour at 24 hours post-treatment.

Before levels of activated caspase activity were determined, whole intact cells were gated using the forward and side scatter detectors. Next, all sub-G1 cells representing post-apoptotic cells and cellular fragments were excluded, in addition to all doublets, triplets and any macromolecules containing more PI-stained DNA than cells in G2. Based analysis of the [FL- PI+] cells, 101 on the FL1-H y-axis, representing intra-cellular FLICA concentration, has been chosen as the threshold value below which any

detected signal can be attributed to background processes either by normal cellular fluorescent activity or detector noise. The double positive controls [FL+PI+] had about 45% of activated caspases 3 and 7 while the drug only [FL+PI+] cells, treated with 7.5 μM of β–Lapachone for 1 hour followed by 24 hours of being drug-free under ideal cell culturing conditions, had about 80% (or about a 78% increase above control level) of activated caspases 3 and 7.

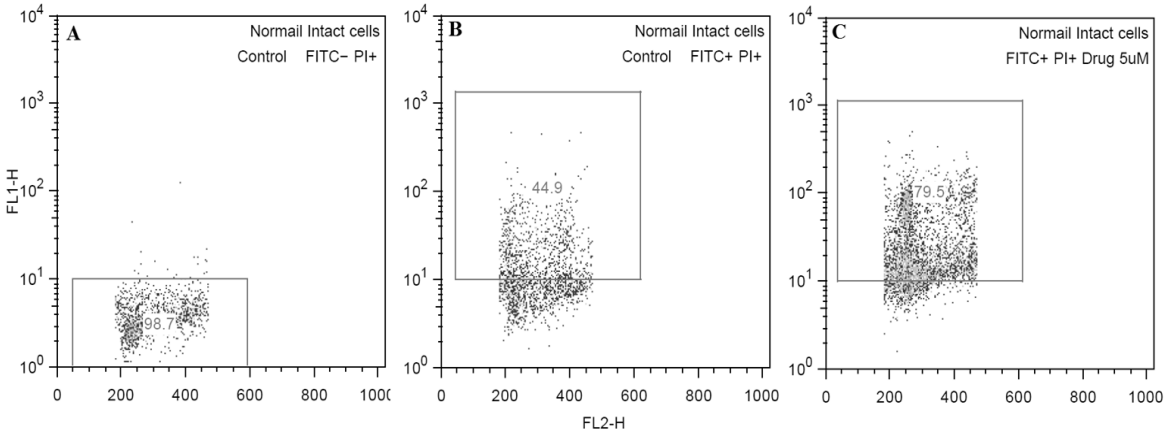

Figure 3.2.e. Graph showing number of detectable FITC events per cell on the FL1-H y-axis, and length of PI stained DNA on the FL2-H axis where just over 200 marks the G1 cell cycle peak. [A.] FITC negative and PI positive whole and intact untreated control cells showing most cells below 101 on the FL1-H FITC y-axis, therefore 10 or fewer detectable FITC events per cell on the FL1-H detector is considered to be background signal. [B.] FITC positive and PI positive whole and intact untreated control cells showing about 45% of the cells having activated caspases 3 and 7. [C.] FITC positive and PI positive whole and intact 7.5 μM β–Lapachone treated control cells showing about 80% of the cells having activated caspases 3 and 7, which is a 78% increase above control levels.

Next, the cell cycle distribution of the double positive controls and the drug treated cells were analytically determined using the Dean-Jet-Fox mathematical modeling algorithm (as described and referenced prior), while having the constraint that G2 needs to have twice as much DNA as G1. Summary of the cell cycle distribution for six independent experiments are presented in Figure 3.2.f.

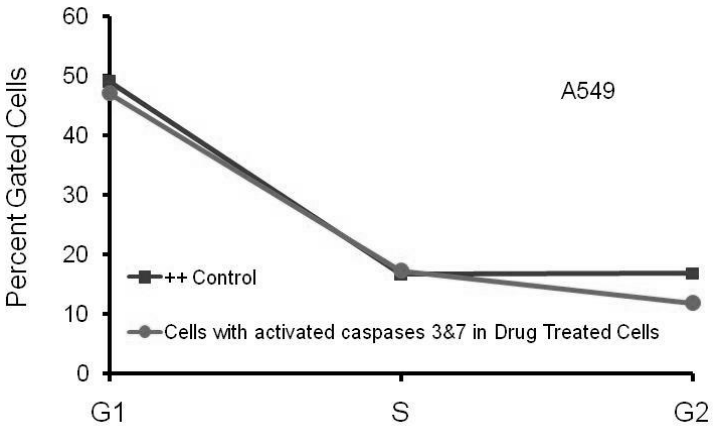

Figure 3.2.f. Comparison of the average percent cell cycle of FITC positive drug treated cells with the average percent cell cycle distribution of double positive untreated controls. N=6. Percent sub G1 not shown.

As can be seen, the cell cycle distribution of the cells in the early stages of apoptosis as determined by levels of activated caspases 3 and 7 is comparable to the cell cycle distribution of untreated controls. Therefore, based on these added results, another conclusion can be drawn from these results:

9. <u>β–Lapachone's cytotoxic effects appears to be cell cycle phase independent.</u>

3.3 Tumor Response

Given that a fraction of tumor cells in vivo are hypoxic cells, the possible differential effect of β–Lapachone between normoxic cells and hypoxic cells were studied in vitro.

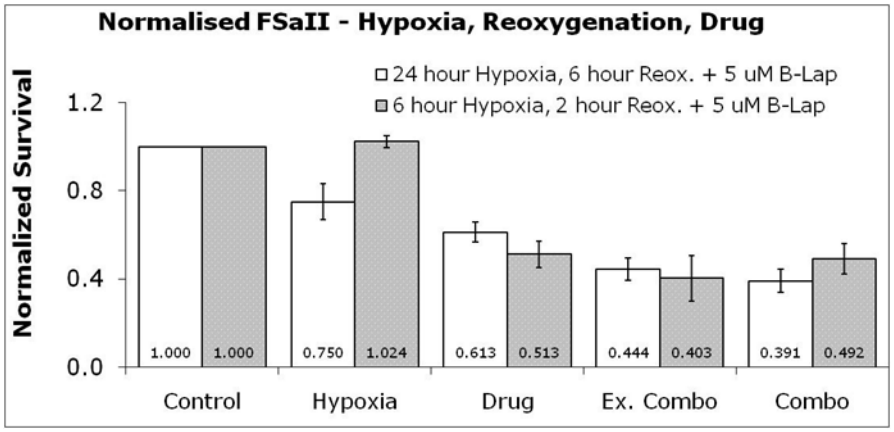

Figure 3.3.a. Normalized survival of A549 cells under normoxic and hypoxic conditions with and without the presence of 5 μM of β–Lapachone. The general agreement between the expected additive effects in the combined treated group and the actual results of the combined treated group suggest that there is no synergy in cell killing between hypoxic cells and β–Lapachone.

For this experiment, creating a hypoxic environment proved to be a challenge. After much experimentation, it was observed that using glass flasks instead of the usual plastic flasks resulted in the best results in creating and maintaining a hypoxic environment for cultured cells. A549 cells were grown on the flat surface of specially designed glass tubes, which provided an elongated culturing surface. Known numbers of cells were seeded and maintained in regular media for 14-16 hours. A sterilized air-tight rubber stopper, used to cover the opening of the glass tube, was perforated by two large

gauged hypodermic needles. A mixture of 95% nitrogen and 5% CO2 air was used to aerate the inside of the tubes through one of the needles while the other needle served as an outlet for neutralizing the pressure within the tubes. Positive flow into the tubes from the 95% nitrogen and 5% CO2 air ensured that there was no backflow of oxygenated ambient air. This air exchange process was done continuously for 30 minutes to ensure a through expulsion of oxygen within the tubes. A visual observation of increased acidity, as a result of anaerobic respiration and lactic acid production, was made by the change in the media color towards light yellow due to the presence of phenolsulfonphthalein (a color pH indicator). Seven groups were established, where each data point for each experiment represents a duplicate of two flasks: a control group receiving no drug and remained in a normoxic environment, two hypoxic groups where one group maintained a hypoxic environment for 6 hours and another maintaining a hypoxic environment for 24 hours, two drug only groups, both receiving 5 μM of β–Lapachone one for 6 hours and the other for 2 hours, and finally a combined group receiving 24 hours of continuous hypoxic environment followed by 6 hours of β–Lapachone at 5 μM, and the other group receiving 6 hours of continuous hypoxic environment followed by 2 hours of β–Lapachone at 5 μM. The tubes were rapidly reoxygenated using a 50 cc gauge syringe to expedite air exchange at the onset of administering the drug. Combined treated groups and drug only groups were treated with 5 μM of β–Lapachone for their respective drug times in an incubator, then all groups were gently rinsed with phosphate buffered saline (PBS) twice before adding supplemented media and returning them to an incubator for about 7-10 days. This experiment was repeated six times for significance. After clonogenicity was determined for each group, data were normalized to controls, as can be

seen in Figure 3.2.c. The expected combined groups "Ex. Combo" was determined by multiplying the fractional survival of the hypoxic groups with the respective drug treated groups. The survival of the actual combined treated groups was in good agreement (with-in each other's respective standard error margins), suggesting that the effects of rapidly reoxygenated cells following a course of chronic hypoxia and the effects of 5 μM of β–Lapachone were only additive.

Based on this result, the following conclusion can be drawn:

10. β–Lapachone's cytotoxicity exhibits no cell killing synergy in vitro with cells that were recently reoxygenated following chronically hypoxic conditions.

Effect of β–Lapachone and X-irradiation on tumors

In order to determine the effect of β–Lapachone on murine tumors, FSaII cells were prepared for inoculation to ~20 gram C3H mice (The Jackson Laboratory, Bar Harbor, Maine). All studies were done in strict accordance of University of Minnesota Institutional Animal Care and Use Committee (IACUC). Exponentially growing cells were harvested and suspended in serum-free medium to a final concentration of $4x10^6$ cells in 1 ml. Each mouse received $2x10^5$ cells in 50 μl subcutaneously into the right hind leg. When tumors grew to a diameter of about 5-7 mm, mice were separated into groups: control, drug only, x-irradiation only and combined drug and x-irradiation treatments. Mice that were treated with drug received an intraperitoneal injection of β–Lapachone

diluted in Hydroxypropyl Beta Cyclodextrin (HPβCD) (60) solution to a concentration sufficient to inject 50 mg/kg of β–Lapachone in 200 µl of cocktail solution. Mice that were x-irradiated were first anesthetized using a cocktail of ketamine (100 mg/kg) and xylazine (10 mg/kg) diluted in sterile saline. We preferred an injectable volume of 0.2 ml per mouse which weighed ~20 gram, so the working solution of 4 ml of ketamine (100 mg/kg) + 2 ml of xylazine (10 mg/kg) + 34 ml sterile saline was used and stored in rubber sealed blood tubes. After mice were anesthetized, they were loaded unto specially designed holders which provided for the tumor bearing legs to be positioned away from the rest of the body and exposed to a single fraction of 20 Gy at a dose-rate of approximately 1.5 Gy/minute. Lead shielding (4 mm thick) was used to protect the mice from the x-irradiation except for the area around the tumor. Analgesics or antibiotics were added to the drinking water post-treatment as warranted to keep the animal condition within the limits of the criteria for euthanasia. Tumor volumes were calculated using the formula:

$$Volume = \frac{a^2 b}{2}$$

Where ‘a’ was the shortest tumor diameter and ‘b’ was the longest tumor diameter measured. Measurements were recorded using a caliper. Tumor volumes were measured every other day and the results were plotted in Figure 3.3.b.

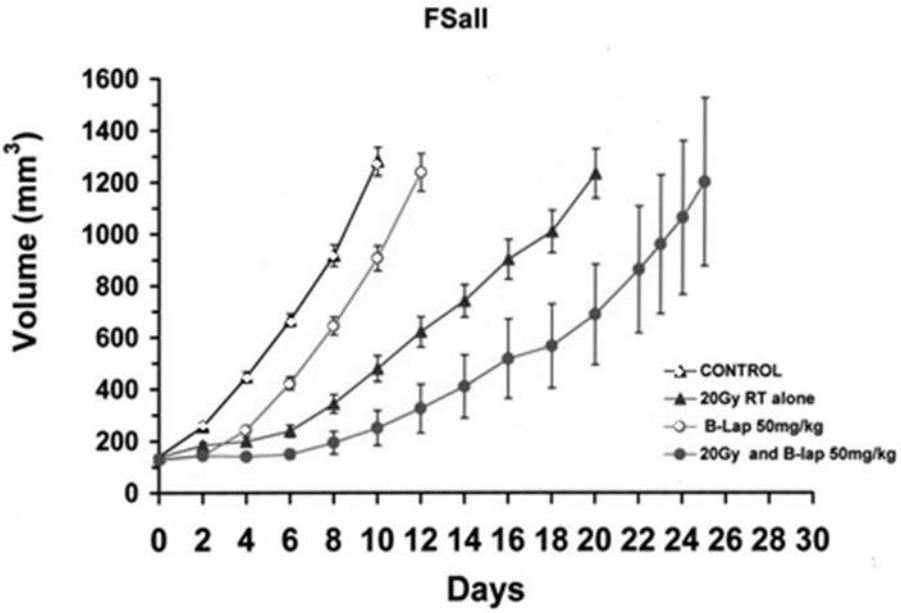

Figure 3.3.b. Growth delay of FSaII tumors grown in C3H mice. Time for the tumor to grow and increase its volume fivefold (or about 800 mm3) was about 7 days in the control, 9 days in the 50 mg/kg of β–Lapachone group, 15 days in the 20 Gy x-irradiation only group and about 22 days in the combined treated group. (Data points are means of 7–10 tumors ± 1 S.E) The difference between the radiation only group and the combined treated group (16 days v.s. 22 days), was statistically significant ($P<0.001$). Source: Compiled experimental data from the Radiation Biology Laboratory at the University of Minnesota.

Untreated control tumors grew in an expected exponential-like manner. Those treated with both 20 Gy of x-irradiation and 50 mg/kg of β–Lapachone showed a marked and sustained delay of growth when compared to tumors treated with either 50 mg/kg of β–Lapachone or 20 Gy only suggesting increased cell killing due to the complimentary mechanisms discussed. However, cells which are most sensitive to radiation within a tumor are the cells that are closest to a reliable blood supply and oxygen, so similarly, the hypoxic cells which are more radio- resistant to radiation treatments are for the same

reason the cells which tend to be out of reach of β-Lapachone. As such, how our tumors responded to a fractionated regimen of β–Lapachone and radiation was of interest. In order to investigate this question, another experiment was repeated to observe the tumor response to fractionated combined treatments. FSaII tumors of about 5-7 mm were divided into four groups: control, fractionated drug only, fractionated x-irradiation only and combined fractionated drug and x-irradiation treatments. The 20 Gy radiation treatments was split into 4 equal parts of 5 Gy each fraction and delivered to the tumor bearing hind legs every other day. 50 mg/kg of β–Lapachone was given to the drug only and the combined treated groups 30 minutes before each radiation treatment. Tumor volumes were measured every other day, on the same days as irradiation. The relative volumes of the tumor growth were determined by dividing the measured volumes for each reading by the initial volumes measured on 'Day 0'. These results were plotted in Figure 3.3.c.

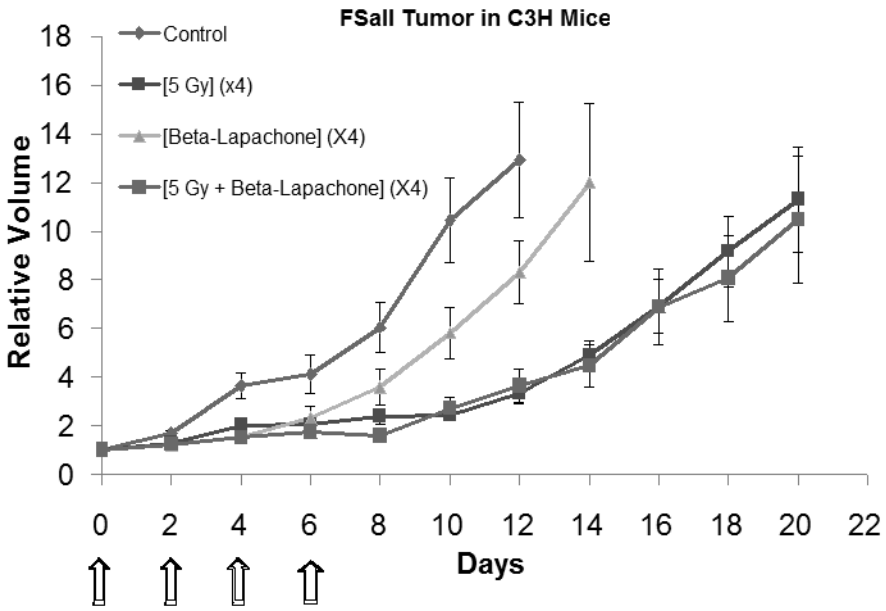

Figure 3.3.c. Tumor growth delay in FSaII tumors grown in C3H mice. Time for

the tumor to have an eightfold increase was about 9 days in the control, 12 days in the 50 mg/kg of β–Lapachone group, and about 16 days for both the 20 Gy (5 Gy x 4 fractions) x-irradiation only group and the combined fractionated treated group. (Data points are means of 7–10 tumors ± 1 S.E). Arrows represent treatment of 5 Gy x-irradiation and 50 mg/kg of β–Lapachone.

As can be seen, an even greater tumor control was not observed for a treatment involving fraction when compared to a single treatment, and was unexpected based on the in vitro studies. Fearing experimental error, this study was very carefully repeated with very similar results. Given that the combined group showed no difference in tumor control than the radiation only group, it was suspected that there was no increased sensitivity due to the fact that the drug was not effective in consecutive treatments. Given that the activating enzyme NQO1 is upregulated upon cellular stress such as ionizating radiation, and consequently potentiates β–Lapachone's cytotoxic effects, perhaps the concentrations of the enzyme is not regenerated in as high numbers as its first cell stressing event, or its concentration is reduced based on its initial interaction with β–Lapachone. In either of those two scenarios, a lower concentration of NQO1 during the second, third and fourth treatments would consequently reduce β–Lapachone's cytotoxic potential. In order to determine if enzymatic activity is affected following an initial treatment of β–Lapachone, an immune western blot study was performed for the detection of NQO1 in a post treated cell. After a through literature search, the predominant focus has been towards treatments which would show an increase in NQO1, as opposed to what happens to the cellular concentrations after a treatment with β–Lapachone.

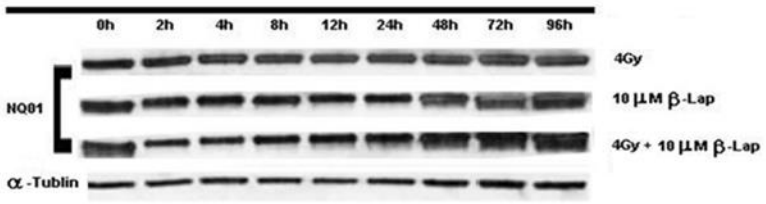

Figure 3.3.d Western blot analysis for NQO1. At 0h, cells that received either 4 Gy or 4 Gy and 10 μM of β– Lapachonewere irradiated. Cells that received either 10 μM of β– Lapachone or 4 Gy and 10 μM of β– Lapachone were then treated with 10 μM of β– Lapachone for 1 hour, washed, and incubated at 37ºC under the standard culture conditions. At the indicated end time points after β–Lapachone treatment, cells were collected for western blot analysis. Blots were labeled with anti-NQO1 antibody and then with a horseradish peroxidase- conjugated secondary antibody, and visualized using chemiluminescence.

Possible NQO1 depletion after treatment with β–Lapachone was studied. The following experiment was performed using A549 cells.

Control		[collect cells]	[Western Blot]
4Gy	[Incubate 2 hours]	[collect cells]	[Western Blot]
4Gy	[Incubate 4 hours]	[collect cells]	[Western Blot]
4Gy	[Incubate 8 hours]	[collect cells]	[Western Blot]
4Gy	[Incubate 12 hours]	[collect cells]	[Western Blot]
4Gy	[Incubate 24 hours]	[collect cells]	[Western Blot]
4Gy	[Incubate 48 hours]	[collect cells]	[Western Blot]
4Gy	[Incubate 72 hours]	[collect cells]	[Western Blot]
4Gy	[Incubate 96 hours]	[collect cells]	[Western Blot]
10 μM (1 hour)	[Rinse then incubate 2 hours]	[collect cells]	[Western Blot]
10 μM (1 hour)	[Rinse then incubate 4 hours]	[collect cells]	[Western Blot]
10 μM (1 hour)	[Rinse then incubate 8 hours]	[collect cells]	[Western Blot]
10 μM (1 hour)	[Rinse then incubate 12 hours]	[collect cells]	[Western Blot]
10 μM (1 hour)	[Rinse then incubate 24 hours]	[collect cells]	[Western Blot]
10 μM (1 hour)	[Rinse then incubate 48 hours]	[collect cells]	[Western Blot]
10 μM (1 hour)	[Rinse then incubate 72 hours]	[collect cells]	[Western Blot]

10 μM (1 hour)	[Rinse then incubate 96 hours]	[collect cells]	[Western Blot]
4Gy + 10 μM (1 hour)	[Rinse then incubate 2 hours]	[collect cells]	[Western Blot]
4Gy + 10 μM (1 hour)	[Rinse then incubate 4 hours]	[collect cells]	[Western Blot]
4Gy + 10 μM (1 hour)	[Rinse then incubate 8 hours]	[collect cells]	[Western Blot]
4Gy + 10 μM (1 hour)	[Rinse then incubate 12 hours]	[collect cells]	[Western Blot]
4Gy + 10 μM (1 hour)	[Rinse then incubate 24 hours]	[collect cells]	[Western Blot]
4Gy + 10 μM (1 hour)	[Rinse then incubate 48 hours]	[collect cells]	[Western Blot]
4Gy + 10 μM (1 hour)	[Rinse then incubate 72 hours]	[collect cells]	[Western Blot]
4Gy + 10 μM (1 hour)	[Rinse then incubate 96 hours]	[collect cells]	[Western Blot]

After cells were collected, a western blot analysis was performed to observe the relative concentrations of NQO1 in the post-treated cells. As has been described previously, the cells were collected and analyzed as discussed prior. The results can be seen in Figure 3.3.d. The cells treated with both 10 μM of β–Lapachone for 1 hour and 4 Gy of irradiation showed marked reduction in NQO1 levels for up to 24 hours, while 10 μM of β–Lapachone for 1 hour alone and 4 Gy of irradiation showed unchanged levels of NQO1 and a slight increase in NQO1 respectively.

Based on these results, the following conclusions can be drawn:

11. β–Lapachone caused murine tumor growth delay. When used with radiation the tumor growth delay was very pronounced indicating that synergistic effects are at play.
12. Fractionated use of β–Lapachone in combination with radiation does not have a potentiating effect.

13. NQO1 levels are depleted immediately after treatment of β–Lapachone and irradiation in A549 cells. Given β–Lapachone's lack of synergy with radiation when fractionated, it may be a better candidate for steriotatic body radiation therapy (SBRT) and steriotatic radiosurgery (SRS) as opposed to prolonged fractionated regimens.

4 Conclusion

The following is a summary of pertinent findings collected through laboratory experimentation, and its implications in treating tumors in combination with therapeutically relevant radiation therapy. Moreover, the following will propose how to lever0age these findings towards developing a new therapeutic alternative using β–Lapachone and therapeutic radiation for the treatment of solid tumors.

4.1 Summary of Findings and Implications

1. β–Lapachone’s cytotoxicity increases with exposure time to the cell, and so is time dependant.
2. β–Lapachone’s cytotoxicity increases with its concentration, and so is not phase specific in vitro.
3. Levels of NQO1 are up-regulated by ionizing radiation of 4 Gy.
4. Levels of NQO1 remains at elevated for more than 72 hours after 4 Gy.
5. There is significant suppression of sublethal damage repair with a nominal treatment of β–Lapachone after the second fraction of radiation; moreover, there is increased sensitivity beyond the suppression of repair, which suggests other cellular mechanisms at play.
6. Suppression of sublethal damage repair is more effective when β–Lapachone is administered following the first fraction of radiation as opposed to the second fraction of radiation, where β–Lapachone's concentration and treatment times are

equal.

7. A population of A549 cells treated with 7.5 μM of β–Lapachone only modestly alters the proportions of cells in the various parts of the cell cycle, such as increased proportion of cells in the S-phase, when compared to untreated cells.
8. There is significant cell cycle arrest in A549 cells after irradiation of 4 Gy within the first 24 hours, however when cells are also under the influence of 7.5 μM of β–Lapachone, there is no discernible arrest in the cell cycle.
9. β–Lapachone's cytotoxic effects appears to be cell cycle phase independent.
10. β–Lapachone's cytotoxicity exhibits no cell killing synergy in vitro with cells that were recently reoxygenated following chronically hypoxic conditions.
11. β–Lapachone caused murine tumor growth delay. When used with radiation the tumor growth delay was very pronounced indicating that synergistic effects are at play.
12. Fractionated use of β–Lapachone in combination with radiation does not have a potentiating effect.
13. NQO1 levels are depleted immediately after treatment of β–Lapachone and irradiation in A549 cells. Given β–Lapachone's lack of synergy with radiation when fractionated, it may be a better candidate for steriotatic body radiation therapy (SBRT) and steriotatic radiosurgery (SRS) as opposed to prolonged fractionated regimens.

Many of the findings are tacitly in agreement with literature, while adding to the body of scientific knowledge. This work clearly demonstrates that the effect of novel

anticancer drug β– Lapachone against mouse FSaII fibrosarcoma and human A549 lung cancer is potentiated by therapeutically relevant radiation. Importantly, we also found that β-lap treatment applied soon after irradiation inhibits the repair of sub-lethal radiation damage (SLD) as demonstrated by the changes in the shape of radiation survival curve. This understanding is based on experiments which shows β–Lapachone-induced SLD repair was inhibited using split-dose radiation studies. Moreover, β–Lapachone inhibition of the repair of sub-lethal damage caused by ionizing irradiation offers a complimentary mechanism which is greater than additive in cell lethality. These findings, as summarized above demonstrate that NQO1 plays central role in the β–Lapachone-induced cell death. On its own, β–Lapachone has cytotoxic effects after it is activated by NAD(P)H:quinine oxidoreductase and then enters into a futile cycling between the original oxidized form of β–Lapachone and its two-electron reduced forms. The cycling between the oxidize and reduced forms of β–Lapachone generates reactive oxygen species (ROS), thereby causing DNA damages, depletion of NAD+ and ATP, Ca2+-dependent PARP-1 hyperactivation, loss of mitochondrial membrane potential, loss of Ca2+ homeostasis, inhibition of NFkB, degradation of p53 and activation of u-calpain (59) (60) (49) (53). NQO1 activity in tumors is significantly higher than those of non-cancerous normal tissues by as much as 100-fold (60) (61) (62), indicating tumors will be preferentially targeted by β–Lapachone's cytotoxic activities. The expression of NQO1 gene is mainly regulated by the antioxidant response element (ARE) and has been shown to be activated by chemical induced oxidative stress, mild temperature hyperthermia and ionizing radiation (54) (55). Unlike radiation, β–Lapachone appears to be cell cycle agnostic in terms of its cytotoxicity, however its action has dramatic control over

radiation induced cell cycle check points, as was observed by the strong corelation between cells treated with β–Lapachone only and β–Lapachone combined with radiation. In addation, the cell cycles of cells treated with β–Lapachone closely mirrors that of untreated control cells. It also appears to be largely unaffected by whether a cell was previously hypoxic or whether a cell have always been in a normoxic environment. Considerations for β–Lapachone‘s cytotoxicity in cells currently under hypoxic conditions were not evaluated due to unfeasibility of the drug reaching the hypoxic cells in a tumor, by the very nature of why some cells are hypoxic. This is in contrast to irradiation studies where cells outside of a sufficiently reliable blood supply are still of consideration when attempting to understand its response to treatments (12). We can additionally elucidate that the response of tumors in vivo to β–Lapachone (i.p. with 50 mg/kg) combined with ionizing radiation (20 Gy) caused tumor growth delays when compared to individual treatments alone. As such, the combined effects were apparently greater than additive. However these benefits vanished when consecutive tumor fractionated studies showed no synergistic benefit to fractionated treatments when compared to a single treatment, moreover, the tumor delaying effect was surprisingly even less than additive. Based on subsequent western blot studies where relative concentrations of NQO1 were observed, it shows a decline in its concentration following combined treatments of β-lap and irradiation, in a treatment comparable to one of the fractionated treatments. Future studies are needed to better characterize NQO1 levels, not only to observe possible ways for its up-regulation, but to also observe its concentration in a post β– Lapachone and a combined β–Lapachone and radiation treated environment. However, based on what was observed, the synergy in cell lethality between β–

Lapachone and therapeutic radiation appears to be best exploited when used in a single fraction, therefore putting it into consideration for used along with SBRT and SRS treatments.

5 Bibliography

1. *A note from history: landmarks in history of cancer, part 1.* **Hajdu SI, Thun, MJ, Hannan, LM, Jemal, A.** 5, 2011, Cancer, Vol. 117, pp. 1097–102.

2. *BASC, a super complex of BRCA1-associated proteins involved in the recognition and repair of aberrant DNA structures.* **Wang Y, Cortez D, Yazdi P, Neff N, Elledge SJ, Qin J.** s.l. : 14, 2000, Genes & Development, Vol. 8, pp. 927–39.

3. *"The BRCA1/2 pathway prevents hematologic cancers in addition to breast and ovarian cancers".* **B, Friedenson.** 152, 2007, BioMed Central Cancer, Vol. 7.

4. *ON A NEW KIND OF RAYS.* **Röntgen, Wilhelm.** 59, 1896, Science, Vol. 3, pp. 227-231.

5. *History of Head and Neck Radiology: Past, Present, and Future.* **Weber, Alfred L.** 2001 : s.n., Radiology, Vol. 218, pp. 15-24.

6. **National Cancer Institute, NIH, DHHS.** *Cancer Trends Progress Report.* 2012. http://progressreport.cancer.gov.

7. **Thomas, Charles C.** *The physics of radiology.* 3rd ed. Springfield : s.n., 1969.

8. **Hall, Eric J and Giaccia, Amato J.** Radiobiology for the Radiologist. [book auth.] Eric J Hall. *Radiobiology for the Radiologist.* 6th. New York : Lippincott Williams & Wilkins, 2006, 1, p. 15.

9. *Apoptosis and cell cycle progression in an acidic environment after irradiation.* **Park H, Lyons JC, Griffin RJ, Lim BU, Song CW.** 3, 2000, Radiatrion Research, Vol. 153, pp. 295-304.

10. *Radiation-induced apoptosis in different pH environments in vitro.* **Lee HS, Park HJ, Lyons JC, et al.** 1997, International Journal of Radiation Oncology * Biology * Physics, Vol. 38, pp. 1079 –1087.

11. *Effect of acidic environment and p53 on apoptosis induction by hyperthermia.* **Ohtsubo T, Park HJ, Lyons JC, Ohnishi T, Song CW.** 6, 2000, International Journal of Hyperthermia , Vol. 16, pp. 481-91.

12. *Acidic environment causes apoptosis by increasing caspase activity.* **H J Park, J C Lyons, T Ohtsubo, and C W Song.** 12, 1999, British Journal of Cancer, Vol. 80.

13. *Apoptosis and perturbation of cell cycle progression in an acidic environment after hyperthermia.* **Takasu T, Lyons JC, Park HJ, Song CW.** 12, 1998, Vol. 58, pp. 2504-8.

14. *DNA strand breaks signal the induction of DNA double-strand break repair in Saccharomyces cerevisiae.* **Sing, R K and Krishna, M.** 2005, Radiation Research, Vol. 164, pp. 781–790.

15. *Repairing Double-Strand DNA Breaks.* **Negritto, Cristina M.** s.l. : Nature Education, 2010, Nature Education .

16. *Radiation Response of Mammalian Cells Grown in Culture: V. Temperature Dependence of the Repair of X-Ray Damage in Surviving Cells (Aerobic and Hypoxic).* **Elkind, M M.** 2, s.l. : Radiation Research, 1965, Vol. 25.

17. *Time effects in molecular radiation Biology.* **Adams, G E.** s.l. : Radiation and Environmental Biophysics, pp. 95-113.

18. *Radiation response of mammalian tumor cells. Repair of sublethal damage in vivo.* **Belli, J A.** Journal of the National Cancer Institute, pp. 673-682.

19. *Reduced Oxygen Enhancement Ratio at Low Doses of Ionizing Radiation.* **Palcic, B.** 2, s.l. : Radiation Research, 1984, Vol. 100, pp. 328-339.

20. *Radiobiological properties of high-energy cyclotron-produced neutrons used for radiotherapy.* **Hall, E J.** s.l. : Radiology, pp. 173-178.

21. *Apoptosis and Cell Cycle Progression in an Acidic Environment after Irradiation.* **HeonJoo Park, John C. Lyons, Robert J. Griffin, Byung U. Lim, and Chang W. Song.** 3, s.l. : Radiation Research, 2000, Vol. 153, pp. 295-304.

22. *Physical Fundations of Radiology.* **Goodwin, P N, Quimby, E H and Morgan, R H.** New York : Harper & Row, 1970.

23. *Neutron and Heavy Particle Dosimetry.* **Rossi, H H.** New York : Academic Press, 1964, Radiation Dosimetry: Proceedings of the International School of Physics, pp. 98-107.

24. *G1 events and regulation of cell proliferatio.* **Pardee, A.** s.l. : Science, 1989, Vol. 246, pp. 603–608.

25. *What is the restriction point?* **Zetterberg, Anders, Larsson, Olle and Wiman, Klas G.** 6, s.l. : Current Opinion in Cell Biology, 1995, Vol. 7, pp. 835–842.

26. **Alberts, Bruce, et al., et al.** Chapter 18 Apoptosis: Programmed Cell Death Eliminates Unwanted Cells. *Molecular Biology of The Cell.* 5th. s.l. : Garland Science, 2008, p. 1115.

27. *The Fas signaling pathway: more than a paradigm.* **H, Wajant.** s.l. : Science, 2002, Vol. 296, pp. 1635–1636.

28. *Lethal toxin of Bacillus anthracis causes apoptosis of macrophages.* **Popov SG, Villasmil R, Bernardi J.** 1, s.l. : Biochemistry Biophysics Research Communication, April 2002, Vol. 292, pp. 349-355.

29. *PARP-1—a perpetrator of apoptotic cell death?* **Chiarugi A, Moskowitz MA.** s.l. : Science, 2002, Vol. 297, pp. 259–263.

30. *Is MAC the knife that cuts cytochrome c from mitochondria during apoptosis?* **Laurent M. Dejean, Sonia Martinez-Caballero, Kathleen W. Kinnally.** s.l. : Cell Death and Differentiation, 2006, Vol. 13, pp. 1387–1395.

31. *Integration of interferon-alpha/beta signalling to p53 responses in tumour suppression and antiviral defence.* **A, Takaoka, et al., et al.** s.l. : Nature, 2003, Vol. 424, pp. 516–523.

32. *Calcium orchestrates apoptosis.* **Chan, Mark P. Mattson and Sic L.** s.l. : Nature Cell Biology, 2003, Vol. 5, pp. 1041-1043.

33. *The oxygen fixation hypothesis: a reevaluation.* **Ewing, D.** s.l. : American Jurnal of Clinical Oncology, 1998, Vol. 4, pp. 355-361.

34. *On the nature of the oxygen effect on X-ray-induced DNA.* **ROOTS, Ruth and SMITH, KENDRIC C.** 5, 1974, International Jurnal of Radiation Biology, Vol. 26, pp. 467-480.

35. *Predicting the effect of temporal variations in po2 on tumor radiosensitivity.* **Kirkpatrick, J P, Cárdenas-Navia, L I and Dewhirst, M W.** 3, s.l. : International Journal of Radiation Oncology Biology Physics, 2004, Vol. 59, pp. 822–833.

36. *Reduced Oxygen Enhancment Ratio At Low Dosesof Ionization Radiation.* **Palcic, B and Skarsgard, L D.** s.l. : Radiation Research, 1984, Vol. 100, pp. 328-339.

37. *Non-transcriptional control of DNA replication by c-Myc.* **Dominguez-Sola D, Ying CY, Grandori C, Ruggiero L, Chen B, Li M, Galloway DA, Gu W, Gautier J, Dalla-Favera R.** s.l. : Nature, Vol. 448, pp. 445–451.

38. *c-Myc recruits P-TEFb for transcription, cellular proliferation and apoptosis.* **Kanazawa, Satoshi and Soucek Laura, Evan Gerard, Okamoto Takashi, Peterlin B Matija.** 36, s.l. : Oncogene, 2003, Vol. 2, pp. 5707–5711.

39. *Tumor hypoxia, drug resistance, and metastases.* **JM, Brown.** 5, 1990, Journal of The National Cancer Institute, Vol. 82, pp. 338-339.

40. *Vascular endothelial growth factor receptor-2: Structure, function, intracellular signalling and therapeutic inhibition.* **Holmes, Katherine, et al., et al.** 10, s.l. : Cellular Signalling, 2003, Vol. 9.

41. *Serum concentrations of vascular endothelial growth factor-D in angiosarcoma patients.* **Amo, Y., et al., et al.** 1, s.l. : British Journal of Dermatology, 2004, Vol. 150.

42. **Chang W. Song, Heonjoo Park, Robert Griffin, and Seymour H. Levitt.** Radiobiology of Stereotatic Radiosurgery and Stereotatic Body Radiation Therapy. [book auth.] S. H. Levitt. *Technical Basis of Radiation Theraphy, Medical Radiology.* s.l. : Springer-Verlag Berlin Heidelberg, 2012.

43. *Radiation-Induced Vascular Damage in Tumors: Implications of Vascular Damage in Ablative Hypofractionated Radiotherapy (SBRT and SRS).* **Heon Joo Park, Robert J. Griffin,**

Susanta Hui, Seymour H. Levitt, and Chang W. Song. 3, 2012, Radiation Research, Vol. 107, pp. 311-327.

44. *NAD(P)H:quinone oxidoreductase 1 (NQO1): chemoprotection, bioactivation, gene regulation and genetic polymorphisms.* **Ross D, Kepa JK, Winski SL, Beall HD, Anwar A, Siegel D.** 1, 2000, Chem Biol Interact., Vol. 129, pp. 77-97.

45. *One-electron-transfer reactions in biochemical systems V. Difference in the mechanism of quinone reduction by the NADH dehydrogenase and the NAD(P)H dehydrogenase (DT-diaphorase).* **Iyanagi, T. and Yamazaki, I.** 2, 1970, BBA - Bioenergetics, Vol. 216, pp. 282-294.

46. *The role of reductive and oxidative metabolism in the toxicity of mitoxantrone, adriamycin and menadione in human liver derived Hep G2 hepatoma cells.* **Grant, S. J. Duthie and M. H.** 4, 1989, British Journal of Cancer, Vol. 60, pp. 566–571.

47. *Detoxification ability and toxicity of quinones in mouse and human tumor cell lines used for anticancer drug screening.* **Djuric, Z., Corbett, Thomas H. and Valeriote, Frederick A.** 1995, Cancer chemotherapy and pharmacology, Vol. 36, pp. 20-26.

48. *Heat-Induced Up-Regulation of NAD(P)H:Quinone Oxidoreductase Potentiates Anticancer Effects of β-Lapachone.* **Heon Joo Park, Eun Kyung Choi, Jihyung Choi, Ki-Jung Ahn, Eun Jung Kim, In-Mi Ji, Yeon Hee Kook, Seung-Do Ahn, Brent Williams, Robert Griffin, David A. Boothman, Chung K. Lee and Chang W. Song.** 2005, Clinical Cancer Research, Vol. 11, p. 8866.

49. *Immunodetection of NAD(P)H:quinone oxidoreductase 1 (NQO1) in human tissues.* **Siegel D, Ross D.** 3-4, 2000, Free Radic Biol Med. , Vol. 29, pp. 246-253.

50. *Isolation of x-ray-inducible transcripts from radioresistant human.* **DAVID A. BOOTHMAN, MARK MEYERS, NINA FUKUNAGAt, AND SAM W. LEE.** 1993, Proc. Natl. Acad. Sci., Vol. 90, pp. 7200-7204.

51. *Modulating endogenous NQO1 levels identifies key regulatory mechanisms of action of β-lapachone for pancreatic cancer therapy.* **Li LS, Bey EA, Dong Y, Meng J, Patra B, Yan J, Xie XJ, Brekken RA, Barnett CC, Bornmann WG, Gao J, Boothman DA.** 2, 2011, Clinical Cancer Research, Vol. 17, pp. 275-285.

52. *Nicotinamide adenine dinucleotide (phosphate): quinone oxidoreductase (DT-diaphorase) as a target for bioreductive antitumor quinones: quinone cytotoxicity and selectivity in human lung and breast cancer cell lines.* **Beall HD, Murphy AM, Siegel D, Hargreaves RH, Butler J, Ross D.** 3, 1995, Molecular Pharmacology , Vol. 48, pp. 499-504.

53. *Resveratrol and 4-hydroxynonenal act in concert to increase glutamate cysteine ligase expression and glutathione in human bronchial epithelial cells.* **Hongqiao Zhang, Albert Shih, Alessandra Rinna, Henry Jay Forman.** 1, 2006, Archives of Biochemistry and Biophysics, Vol. 481, pp. 110-115.

54. *Anti-cancer effect of bio-reductive drug beta-lapachon is enhanced by activating NQO1 with heat shock.* **Song CW, Chae JJ, Choi EK, Hwang TS, Kim C, Lim BU, Park HJ.** 2, 2008, International Journal of Hyperthemia , Vol. 24.

55. *Pharmacological Stimulation of NADH Oxidation Ameliorates Obesity and Related Phenotypes in Mice.* **Jung Hwan Hwang, Dong Wook Kim, Eun Jin Jo, Yong Kyung Kim, Young Suk Jo, Ji Hoon Park, Sang Ku Yoo, Myung Kyu Park, Tae Hwan Kwak, Young Lim Kho, Jin Han, Hueng-Sik Choi, Sang-Hee Lee, Jin Man Kim, InKyu Lee, Taeyoon Kyung, Cholsoon Jang.** 4, 2009, Diabetes , Vol. 58, pp. 965-974.

56. *Cancer therapy with beta-lapachone.* **Pardee AB, Li YZ, Li CJ.** 3, 2002, Current Cancer Drug Targets, Vol. 2, pp. 227-42.

57. *Activation of a cysteine protease in MCF-7 and T47D breast cancer cells during ß-lapachone-mediated apoptosis.* **Pink JJ, Wuerzberger-Davis S, Tagliarino C, Planchon SM, Yang XH, Froelich CJ, Boothman DA.** 2000, Experimental Cell Research, Vol. 255, pp. 144-155.

58. *Calcium is a key signaling molecule in beta-lapachone-mediated cell death.* **Tagliarino C, Pink JJ, Dubyak GR, Nieminen AL, Boothman DA.** 22, 2001, The Journal of Biological Chemistry, Vol. 276.

59. *Cisplatin enhances the anticancer effect of b-lapachone.* **Kaoru Terai, Guang-Zhi Dong, Eun-Taex Oh, Moon-Taek Park, Yeunhwa Gu, Chang Won Song and Heon Joo Park.** 10, 2009, Anti-Cancer Drugs, Vol. 20, pp. 901–909.

60. *Enhancement of solubility and bioavailability of B-lapachone using cyclodextrin inclusion complexes.* **Nasongkla N, Wiedmann AF, Bruening A, et al.** 2003, Pharmaceutical Research, Vol. 20, pp. 1626–1633.

61. *AAPM protocol for 40–300 kV x-ray beam dosimetry.* **Ma CM, Coffey CW, DeWerd LA, Liu C, Nath R, Seltzer SM, Seuntjens JP.** 6, s.l. : American Association of Physicists in Medicine, 2001, Medical Physics, Vol. 28, pp. 868-93.

62. **ICRU.** *Radiation Quantities and Units.* Washington, DC : International Commission on Radiation Units and Measurements, 1980. Report No. 33.

63. *Hyperthermia enhances the effect of β-lapachone to cause γH2AX formations and cell death in human osteosarcoma cells.* **Hori, Takeshi, et al., et al.** 1, 2011, International Journal of Hyperthermia, Vol. 27, pp. 53-62.

64. *The effect of mild temperature hyperthermia on tumour hypoxia and blood perfusion: relevance for radiotherapy, vascular targeting and imaging.* **Sun X, Xing L, Ling CC, Li GC.** 3, 2010, International Journal of Hyperthermia, Vol. 26, pp. 224-31.

6 Appendix

6.1 Supplementary Figures

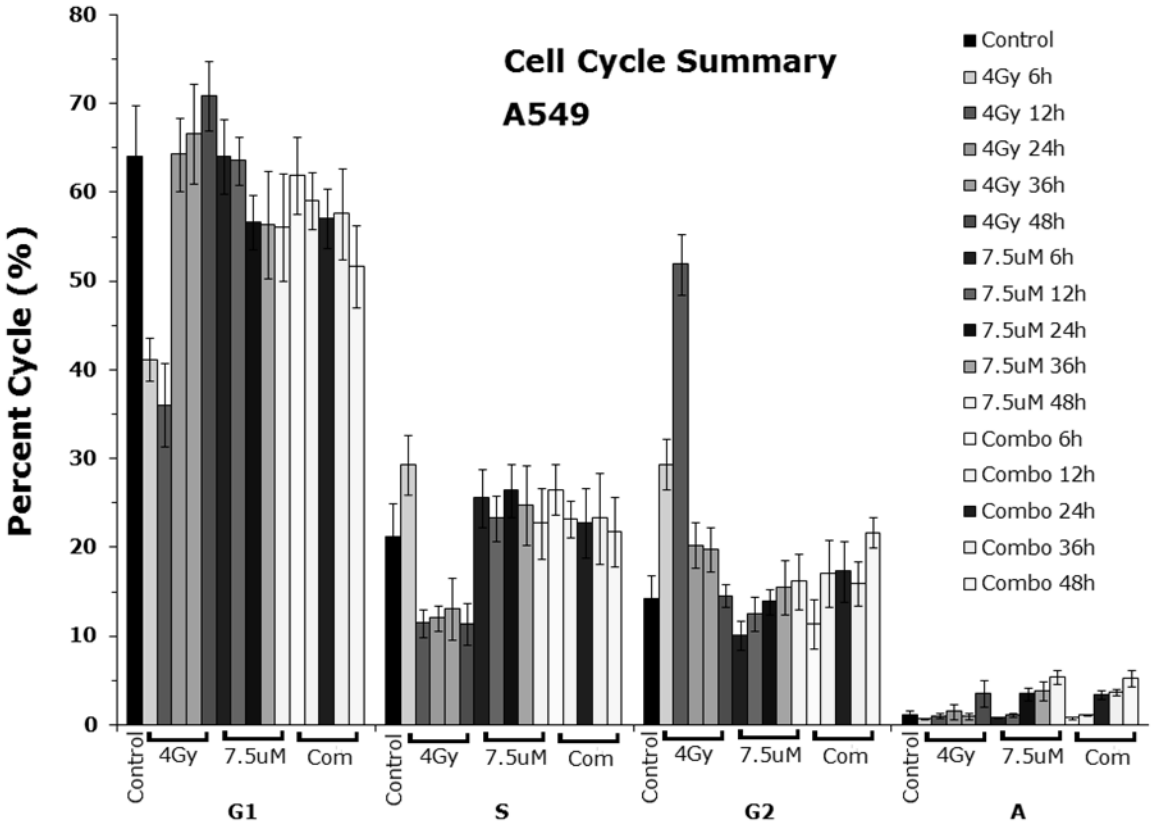

Figure A1 Percent of A549 cells in different cell cycle phases after various treatments with 7.5 μM β–Lapachone and 4 Gy irradiation having various end time points. Percentage of cells in the different cycles were determined by Propidium Iodide intensity staining and calculated using the Dean-Jet-Fox mathematical model. Each data point represents an average minimum of 6 experiments with ± 1 S.E.

Figure A2. Left: A Lapachone tree. Right: Bark extract from the Lapachone tree – used as a medicinal tea. (Wikipedia Commons Image Database)

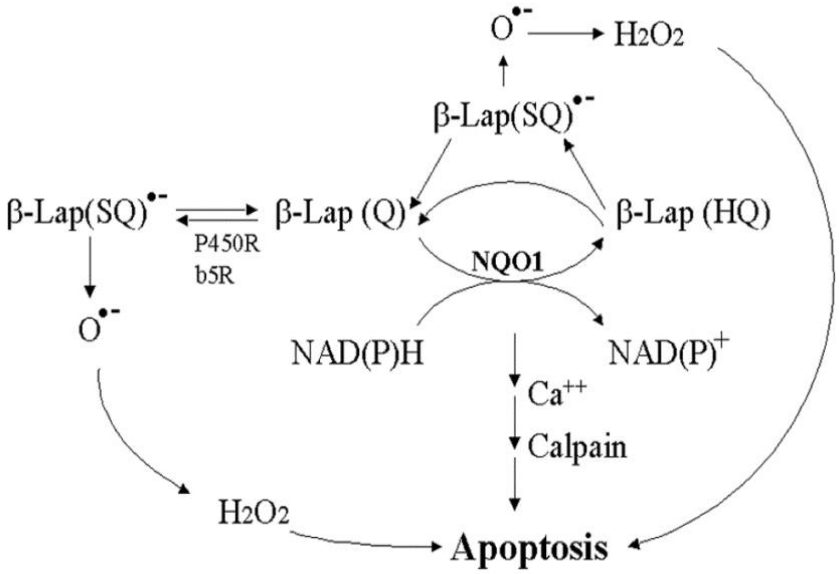

Figure A3. Proposed mode of action for β–Lapachone's cytotoxicity.

6.2 Radiation Dosimetry – TG 61 Work Sheet

Calculating dose to water on phantom surface (61)

Name: **Date:**

(1) X-ray unit: , Tube potential: kV, HVL: mm (Al or Cu)
SSD: cm, Field size: cm^2

(2) Ion chamber and electrometer calibration. Date of last calibration:

Ion chamber: , Calibration factor N_K = Gy/C

Electrometer: , Calibration factor P_{elec} = C/scale unit

(3) Chamber signal: M_{raw} = scale units

(4) Temperature $T=$ °C, Pressure P = $\text{kPa}\left(=\text{mm Hg}\cdot\frac{101.33}{760.0}\right)$

To normalize to 22 °C and 1 atm:

$$P_{TP}=\frac{273.2+T[^\circ\text{C}]}{295.2}\cdot\frac{101.33}{P[\text{kPa}]} \quad =$$

(5) Total radiation time: $t=$ min, end effect: δt = min

(6) Recombination correction $P_{ion}=\dfrac{1-\left(\frac{V_H}{V_L}\right)^2}{\frac{M^H_{raw}}{M^L_{raw}}-\left(\frac{V_H}{V_L}\right)^2}$ =

(7) Polarity correction $P_{pol}=\left|\dfrac{M^+_{raw}-M^-_{raw}}{2M_{raw}}\right|$ =

(8) Corrected chamber reading $M=M_{raw}P_{elec}P_{TP}P_{ion}P_{pol}$ = C

(9) Backscatter factor (Table V, Table VI): B_w =

(10) Mass energy-absorption coefficient ratio water to air (Table IV):

$$\left[\left(\frac{\bar{\mu}_{en}}{\rho}\right)^w_{air}\right]_{air} \quad =$$

(11) Stem correction in air (Sec. V C): $P_{stem,air}$ =

(12) Dose to water: $D_w=MN_KB_wP_{stem,air}\left[\left(\frac{\bar{\mu}_{en}}{\rho}\right)^w_{air}\right]_{air}$ = Gy

(13) Dose rate: $D_w=\dfrac{D_w}{t+\delta t}=$ Gy/min